Received: 30 December 2019 | Revised: 28 February 2020 | Accepted: 17 March 2020

DOI: 10.1002/ardp.201900383

FULL PAPER

DPhG ARCH PHARM Archiv der Pharmazie

Sulfonamides incorporating ketene *N*,*S*-acetal bioisosteres as potent carbonic anhydrase and acetylcholinesterase inhibitors

Qëndresa Istrefi[1] | Cüneyt Türkeş[2] | Mustafa Arslan[3] | Yeliz Demir[4] | Arleta R. Nixha[1] | Şükrü Beydemir[5] | Ömer İ. Küfrevioğlu[6]

[1]Department of Chemistry, Faculty of Mathematical and Natural Sciences, University of Prishtina, Prishtina, Republic of Kosovo,

[2]Department of Biochemistry, Faculty of Pharmacy, Erzincan Binali Yıldırım University, Erzincan, Turkey

[3]Department of Chemistry, Faculty of Arts and Sciences, Sakarya University, Sakarya, Turkey

[4]Department of Pharmacy Services, Nihat Delibalta Göle Vocational High School, Ardahan University, Ardahan, Turkey

[5]Department of Biochemistry, Faculty of Pharmacy, Anadolu University, Eskişehir, Turkey

[6]Department of Chemistry, Faculty of Sciences, Atatürk University, Erzurum, Turkey

Correspondence

Cüneyt Türkeş, Department of Biochemistry, Faculty of Pharmacy, Erzincan Binali Yıldırım University, Erzincan 24100, Turkey.
Email: cuneyt.turkes@erzincan.edu.tr

Mustafa Arslan, Department of Chemistry, Faculty of Arts and Sciences, Sakarya University, Sakarya, 54187, Turkey.
Email: marslan@sakarya.edu.tr

Funding information

Research Fund of Erzincan Binali Yildirim University, Grant/Award Number: FBA-2017-501; Research Fund of Anadolu University, Grant/Award Number: 1610S681; Research Fund of Sakarya University, Grant/Award Number: 2016-02-04-018

Abstract

In this study, 15 novel compounds in a series of sulfonamide-based ketenes (**7a**–**o**) were synthesized and characterized using Fourier-transform infrared spectroscopy, nuclear magnetic resonance spectroscopy, and mass spectrometry. All compounds were tested for their ability to inhibit the human carbonic anhydrase (*h*CA) isoforms I and II, and acetylcholinesterase (AChE). The halogen-appended compounds, **7g**, **7o**, and **7i**, exhibited the highest *h*CA I/II and AChE inhibition, with the K_I values in the low nanomolar range (K_I = 9.01 ± 0.08, 7.41 ± 0.03, and 7.37 ± 0.31 nM, respectively), as compared with their corresponding parent 2-[2,2-dicyano-1-(phenylamino) vinylthio]-*N*-(4-sulfamoylphenyl)acetamide analogs **7a**–**o**. Besides, derivatives **7c** and **7e** selectively inhibited the isoform *h*CA I, whereas compounds **7m** and **7n** selectively inhibited isoform *h*CA II. These findings indicated that all compounds can inhibit metabolic dysfunctions, such as edema, epilepsy, glaucoma, and Alzheimer's disease, by specifically targeting both the *h*CA isoforms and AChE expression. Herein, also the interactions between ligands and receptors were highlighted through in silico molecular docking studies. The molecular mechanics–generalized Born surface area method was utilized to compute the binding free energy and the energy contribution of the critical residues in the active site was estimated. All these results would help us to perfectly understand the relationship between activity and structural characteristics of derivatives and to further improve newly and highly effective analogs targeting *h*CA and AChE.

KEYWORDS

acetylcholinesterase, carbonic anhydrase, ketene *N*,*S*-acetal, molecular docking, sulfonamide

1 | INTRODUCTION

Electron-donating and -accepting groups containing alkenes, which are called push–pull alkenes, are very important in organic synthesis and synthetic intermediates. Among the ketene acetal compounds, ketene *N*,*S*-acetal is the biggest family, and it is utilized in cyclization and multicomponent reactions for the synthesis of various fused heterocyclic systems and the concerned natural products. Significantly, the reactivity and performance of ketene *N*,*S*-acetals are different and prominent as compared with ketene *O*,*O*-, *N*,*N*-, *S*,*S*-, and

Abbreviations: AAZ, acetazolamide; ACh, acetylcholine; AChE, acetylcholinesterase; AD, Alzheimer's disease; ADMET, adsorption, distribution, metabolism, excretion, and toxicity; CA, carbonic anhydrase; MM–GBSA, molecular mechanics–generalized Born surface area; SAR, structure–activity relationship; TAC, tacrine.

N,O-acetals.[1–3] Thiazolidinones that possess many biological activities were synthesized from ketene *N*,*S*-acetals,[4,5] together with thienopyrroles that have interesting biological properties.[6] Some nucleic acid bases and vitamins that are physiologically important are pyrimidine derivatives,[7] and anilinopyrazolo[1,5-*a*]pyrimidine analogs were synthesized from *S*,*S* and *N*,*S*-acetals, and they are used as c-Src kinase inhibitors for the treatment of acute ischemic stroke.[8] Furthermore, cyclic ketene *N*,*S*-acetal derivatives, ralitoline and etozolin, are used as drugs in the treatment of hypertension and neurological diseases.[9] Nithiazine was the first lead structure of neonicotinoid insecticides and it is widely used as an insecticide in the world.[10,11] Thiazole orange and SYBR safe are the widely utilized probes for nucleic acids in G-quadruplex.[12,13]

Sulfonamides are $-SO_2NH-$ functional group-containing compounds, and they play a significant role in medicinal chemistry. The derivatives of sulfonamide form an important class of sulfur-containing compounds having primary, secondary, and tertiary amides.[14] Sulfonamides resembling 4-amino benzoic acid were discovered in the early 1930s as the first synthetic antibacterial agent, which was the first effective agent against most Gram-positive and many Gram-negative organisms; also, it was employed for bacterial infections.[15,16] Their applications have been further extended as therapeutic agents to treat other diseases. Due to the SO_2NH_2 moiety, sulfamide and sulfamic acid are responsible for binding to the Zn(II) ion within carbonic anhydrase (CA; EC 4.2.1.1) binding site.[17] Sulfonamides have shown several interesting biological activities, including inhibition of CA (acetazolamide, AAZ),[18] anticancer activity (agent E7070),[19] antibacterial activity (sulfathiazole),[20] and HIV protease inhibitory activity.[21] Furthermore, these compounds are a significant class of drugs with several types of pharmacological agents having antitumor, CA inhibitory activity, antidiabetic, diuretic, hypoglycemic, antithyroid, or protease inhibitory activity, as reported in pharmacological and clinical studies.[22] There are many clinically used sulfonamide compounds, for instance, AAZ and brinzolamide as a CA inhibitor for the treatment of glaucoma and seizures,[23,24] benzothiadiazine and chlorothiazide for diuretic activity,[25] hydroflumethiazide for chronic vascular hypertension,[26] benzthiazide for high blood pressure as well as edema,[27] diazoxide for potassium channel activation,[28] and polythiazide for the treatment of congestive heart failure, hypertension, diabetes insipidus, renal tubular acidosis, edema, and the prevention of kidney stones.[29]

Alzheimer's disease (AD) is an irreversible neurodegenerative disease[30] that is known to be the most common type of dementia,[31] accounting for approximately 60–80% of all cases in the world.[32] Acetylcholinesterase (AChE) is an important type of cholinesterase[33] that is responsible for the regulation[34] and degradation[35] of acetylcholine (ACh) in the central nervous system. An increment in ACh expression in the metabolism, owing to the inhibition of the AChE enzyme, leads to the enhancement of the cognitive abilities[36] such as language skills, attention span, and memory functions in AD.[37] Thus, the development of effective AChE inhibitors (AChEIs) may be a critical approach for AD treatment and for preventing the adverse reactions such as digestive tract and hepatotoxicity reactions,[38] which severely affect therapeutic targets induced by AChEIs during treatment.

CAs, are the metalloenzymes, have a crucial role in many metabolic processes like bone resorption,[39] calcification,[40] carboxylation,[41] photosynthesis,[42] pH regulation,[43] respiration,[44] and ureagenesis,[45] etc and catalyzing the CO_2 hydration/dehydration biochemical reaction a reversible.[46,47] Although human CAs belong to the α-class, they are classified into seven different families[48]: α-, β-, γ-, δ-, ζ-, η-, and θ-CA. Human carbonic anhydrase I and II (*h*CA I/II) are cytosolic isoforms,[49] and irregular or overexpression of these enzymes is associated with some pathological disorders. *h*CA I isoenzyme is correlated with retinal and cerebral edema,[50] whereas *h*CA II isoform is associated with edema,[51] epilepsy,[52] and glaucoma.[53] Thus, *h*CAs are an important drug target enzyme, and several CA inhibitors are currently in clinical use in different pharmaceutical forms. Therefore, the design and synthesis of novel inhibitors with high-order isoform selectivity index is an excellent approach to contribute to the field of toxicology with drug discovery and development technology. In this context, CA inhibitors, mainly sulfonamides, are the most targeted and researched ligands in drug design because they are effectively zinc-binders. The sulfonamides are especially known as dual CA and AChE inhibitors. On the basis of the above information, we focused on the design and synthesis of 15 new ketene *N*,S-acetal sulfonamides (**7a–o**) displaying selectivity as CA inhibitors. We appended differently substituted functional groups, such as fluorine, chlorine, bromine, iodine, methyl, methoxy, and nitro, as a tail to the heterocyclic scaffolds of compounds to maximize the interaction of derivatives with the binding sites of *h*CA isoforms I, II, and AChE, and researched their in vitro and in silico biological effects on these enzymes. Furthermore, we extended this study to understand the structure–activity relationships (SARs) of this class of analogs.

2 | RESULTS AND DISCUSSION

2.1 | Chemistry

A new series of ketene *N*,*S*-acetal sulfonamide compounds (**7a–o**) was synthesized, and it is presented in Schemes 1 and 2. Chloroacetylchloride-substituted sulfonamide (**3**) was prepared from sulfanilamide and acetylchloride in the presence of triethylamine (TEA) in dimethylformamide (DMF) at 0°C for 5 hrs. The ketene *N*,*S*-acetal potassium salt was synthesized from isothiocyanate compounds (**4**) and malononitrile with potassium hydroxide in DMF. The targeted compounds were prepared from the ketene *N*,*S*-acetal potassium salt and acetylchloride-substituted sulfonamide in DMF at room temperature. The prepared analogs were characterized by Fourier-transform infrared spectroscopy, ^{1}H NMR (nuclear magnetic resonance), ^{13}C NMR, and elemental analysis.

From the ^{1}H NMR spectra, N–H hydrogen atoms' resonance is observed at 10.60 and 10.80 ppm, sulfanilamide NH_2 hydrogen atoms' resonance is observed at around 7.30 ppm, and resonance of

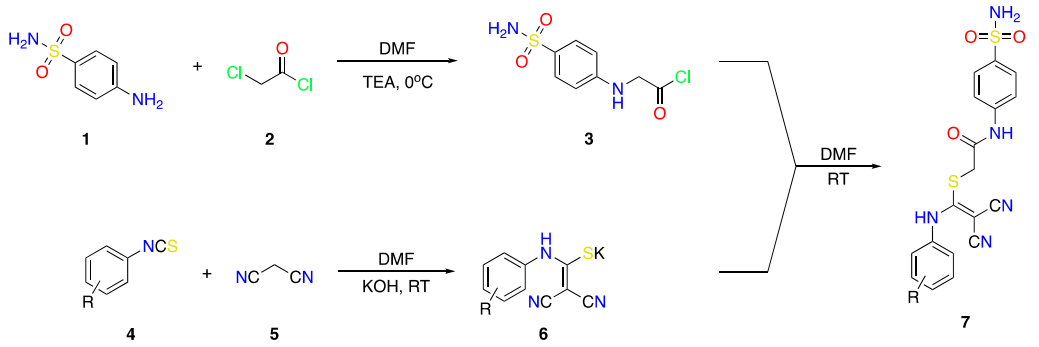

SCHEME 1 General synthetic procedure for target compounds

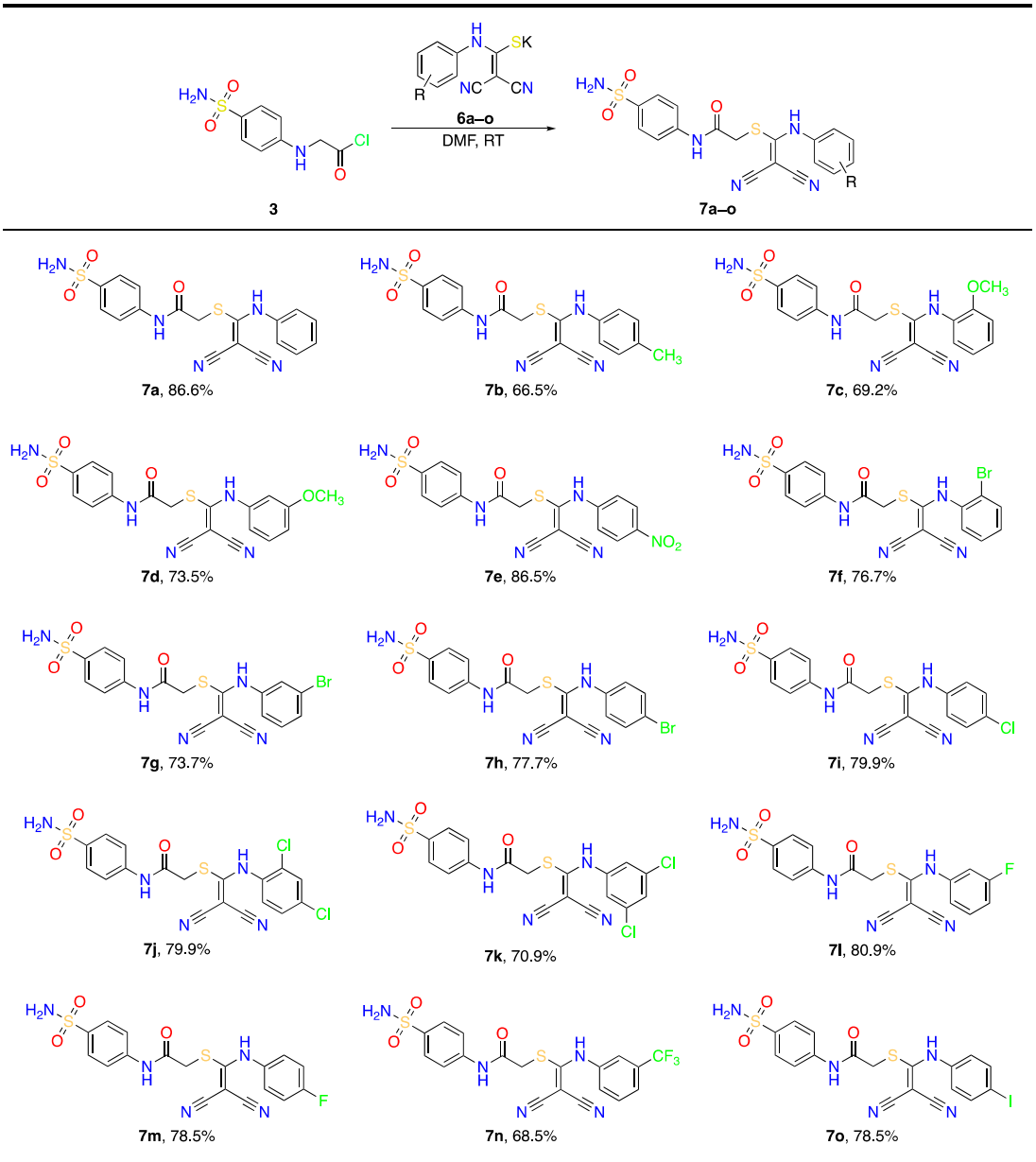

SCHEME 2 Synthesis of ketene *N*,*S*-acetal-substituted sulfonamide derivatives **7a–o** from the compounds **6a–o** and the acetylchloride-substituted sulfonamide **3**

CH_2 hydrogen atoms attached to a sulfur atom is observed at around 4.10 ppm. From the ^{13}C NMR spectra, the resonance of carbonyl carbon atoms is observed at around 167 ppm, and for an SCH_2 carbon atom, it is observed at around 38 ppm. In the infrared spectra of compounds **7a–o**, it was possible to observe the absorptions between 3,200 and 3,350 cm^{-1}, corresponding to NH and NH_2 peaks. Nitrile and amide carbonyl peaks are seen around 2,220 and 1,660–1,700 cm^{-1}, respectively. As seen in the literature,[54] there are two peaks assigned to S═O, symmetric and asymmetric stretching, that are observed around 1,330 and 1,150 cm^{-1}. All spectra and elemental analyses support the structure of the synthesized compounds.

2.2 | Biological evaluation

The newly synthesized 15 sulfonamides, **7a–o,** as detailed above, were screened against physiologically significant cytosolic isoforms *h*CA I, II (associated with some complications like edema and glaucoma, especially), and AChE (associated with AD) for their efficacy as both CA inhibitors and AChE inhibitors by using the esterase and Ellman's assay methods. The standard inhibitors, AAZ and tacrine (TAC), were used as a reference for *h*CA isoforms and AChE in the tests, respectively. According to the data summarized in Tables 1–3, it is revealed that all derivatives are potent inhibitors against *h*CA I, II, and AChE. The SARs of compounds were generated from the inhibition data (IC_{50} values, K_I values, and inhibition types) listed in the tables.

All the newly synthesized ketene *N*,*S*-acetal sulfonamides, **7a–o**, inhibited cytosolic isoform *h*CA I, which is found everywhere and known to be linked with edema, in a potent way, with IC_{50} values ranging from 11.47 ± 0.27 to 31.20 ± 0.41 nM and K_I values ranging from 9.01 ± 0.08 to 107.43 ± 7.76 nM. Furthermore, all analogs showed the best inhibition, compared to AAZ, which is a standard reference drug, and they were found to be more effective inhibitors in the fold between 4 and 52, as compared with AAZ (K_I 475.55 ± 10.62 nM). Compound **7g** (2-[1-(3-bromophenylamino)-2,2-dicyanovinylthio]-*N*-(4-sulfamoylphenyl)acetamide) bearing a 3-bromine showed the best inhibition (K_I 9.01 ± 0.08 nM). The replacement of the 3-methoxy (**7d**, K_I 27.31 ± 0.32 nM), 3-fluorine (**7l**, K_I 16.64 ± 0.16 nM), and 3-trifluoromethyl (**7n**, K_I 22.43 ± 0.50 nM) moieties with a chlorine atom (compound **7g**) led to a reduction in the inhibition. Furthermore, the displacement of the bromine from position 3 to positions 2 and 4 also decreased the inhibition (**7f** and **7h**, K_Is 107.43 ± 7.76 and 96.92 ± 7.19 nM, respectively). On the contrary, the presence of two chlorine atoms (compounds **7j,k**, K_Is 12.16 ± 0.10 and 21.04 ± 0.20 nM, respectively) produced an increase in the inhibition when compared to both **7f** and **7h** derivatives. The replacement of the 3-bromine of compound **7g** with a methyl, nitro, chlorine, fluorine, and iodine groups (analogs **7b**, **7e**, **7i**, **7m**, and **7o**,

TABLE 1 IC_{50} values of *h*CA isoforms (I–II) and AChE with compounds **7a–o**, AAZ, and TAC

	*h*CA I		*h*CA II		AChE	
Compound ID	IC_{50} (nM)	R^2	IC_{50} (nM)	R^2	IC_{50} (nM)	R^2
7a	23.75 ± 0.29	0.9983	12.81 ± 0.05	0.9998	24.37 ± 0.38	0.9986
7b	25.45 ± 0.43	0.9974	14.24 ± 0.14	0.9992	19.32 ± 0.58	0.9967
7c	17.17 ± 0.10	0.9996	17.74 ± 0.27	0.9987	9.77 ± 0.13	0.9983
7d	31.20 ± 0.41	0.9991	19.88 ± 0.27	0.9985	15.59 ± 0.34	0.9942
7e	18.95 ± 0.28	0.9989	15.09 ± 0.16	0.9991	9.39 ± 0.23	0.9963
7f	16.29 ± 0.07	0.9998	16.94 ± 0.22	0.9971	15.76 ± 0.33	0.9959
7g	11.47 ± 0.27	0.9942	8.44 ± 0.06	0.9997	13.96 ± 0.27	0.9951
7h	15.79 ± 0.40	0.9969	15.12 ± 0.11	0.9991	16.36 ± 0.08	0.9999
7i	11.90 ± 0.05	0.9999	13.90 ± 0.18	0.9978	6.81 ± 0.11	0.9988
7j	15.01 ± 0.53	0.9947	10.86 ± 0.05	0.9998	9.34 ± 0.12	0.9977
7k	22.76 ± 0.12	0.9998	18.59 ± 0.19	0.9994	15.88 ± 0.18	0.9981
7l	25.96 ± 0.18	0.9996	14.55 ± 0.21	0.9973	15.16 ± 0.16	0.9986
7m	21.15 ± 0.21	0.9992	14.60 ± 0.16	0.9992	12.73 ± 0.11	0.9993
7n	15.22 ± 0.34	0.9973	8.83 ± 0.14	0.9982	14.76 ± 0.23	0.9987
7o	12.65 ± 0.20	0.9979	10.07 ± 0.25	0.9968	10.54 ± 0.08	0.9995
AAZ	223.90 ± 3.91	0.9988	96.67 ± 0.55	0.9999	–	–
TAC	–	–	–	–	430.10 ± 1.45	0.9998

Abbreviations: AAZ, acetazolamide; AChE, acetylcholinesterase; *h*CA, human carbonic anhydrase; TAC, tacrine.

TABLE 2 Inhibition data of *h*CA isoforms (I–II) and AChE with compounds **7a–o**, AAZ, and TAC

	*h*CA I		*h*CA II		AChE	
Compound ID	K_I (nM)	R^2	K_I (nM)	R^2	K_I (nM)	R^2
7a	22.60 ± 0.22	0.9999	24.14 ± 0.57	0.9999	22.18 ± 0.52	0.9989
7b	23.42 ± 0.23	0.9999	10.53 ± 0.17	0.9999	22.62 ± 1.07	0.9995
7c	48.28 ± 1.40	0.9999	13.07 ± 0.19	0.9999	12.70 ± 0.66	0.9994
7d	27.31 ± 0.32	0.9998	17.59 ± 0.10	0.9999	23.68 ± 1.56	0.9993
7e	105.94 ± 7.12	0.9999	19.46 ± 0.16	0.9999	22.14 ± 2.47	0.9985
7f	107.43 ± 7.76	0.9999	33.58 ± 0.62	0.9999	10.84 ± 0.16	0.9996
7g	9.01 ± 0.08	0.9999	12.58 ± 0.22	0.9999	17.40 ± 0.92	0.9993
7h	96.92 ± 7.19	0.9999	54.65 ± 0.87	0.9999	15.07 ± 0.35	0.9989
7i	20.12 ± 0.48	0.9999	32.35 ± 0.67	0.9999	7.37 ± 0.31	0.9995
7j	12.16 ± 0.10	0.9999	24.60 ± 0.31	0.9999	12.23 ± 0.93	0.9988
7k	21.04 ± 0.20	0.9999	16.09 ± 0.06	0.9999	18.94 ± 1.50	0.9984
7l	16.64 ± 0.16	0.9999	17.84 ± 0.12	0.9999	29.69 ± 3.10	0.9985
7m	21.41 ± 0.46	0.9999	56.75 ± 0.20	0.9999	15.23 ± 0.60	0.9996
7n	22.43 ± 0.50	0.9999	49.92 ± 2.42	0.9999	11.16 ± 0.54	0.9993
7o	16.30 ± 0.44	0.9998	7.41 ± 0.03	0.9999	32.89 ± 5.14	0.9982
AAZ	475.55 ± 10.62	0.9989	97.73 ± 1.62	0.9993	–	–
TAC	–	–	–	–	159.64 ± 0.87	0.9999

Abbreviations: AAZ, acetazolamide; AChE, acetylcholinesterase; *h*CA, human carbonic anhydrase; TAC, tacrine.

TABLE 3 Selectivity index values for K_I constants of the compounds **7a–o**

Compound ID	K_I (*h*CA II/ *h*CA I)	K_I (AAZ/ *h*CA I)	K_I (AAZ/ *h*CA II)	K_I (TAC/ AChE)
7a	1.07	21.04	4.05	7.20
7b	0.45	20.31	9.28	7.06
7c	0.27	9.85	7.48	12.57
7d	0.64	17.41	5.56	6.74
7e	0.18	4.49	5.02	7.21
7f	0.31	4.43	2.91	14.73
7g	1.40	52.78	7.77	9.17
7h	0.56	4.91	1.79	10.59
7i	1.61	23.64	3.02	21.66
7j	2.02	39.11	3.97	13.05
7k	0.76	22.60	6.07	8.43
7l	1.07	28.58	5.48	5.38
7m	2.65	22.21	1.72	10.48
7n	2.23	21.20	1.96	14.30
7o	0.45	29.17	13.19	4.85

Abbreviations: AAZ, acetazolamide; AChE, acetylcholinesterase; *h*CA, human carbonic anhydrase; TAC, tacrine.

K_Is ranging between 16.30 ± 0.44 and 105.94 ± 7.12 nM) also induced a decrease in the inhibition. Thus, in the ketene *N*,*S*-acetal sulfonamides, the inhibitory activity is related to the presence of substituents on the aryl ring; as a matter of fact, compound **7f** displayed the lowest inhibition in this new series. The best derivative was **7g**, bearing a 3-bromine group. The activities for the substituted ketene *N*,*S*-acetal-based sulfonamides (**7a–o**) against *h*CA I were reduced in the following order: **7g** > **7i** > **7o** > **7j** > **7n** > **7h** > **7f** > **7c** > **7e** > **7m** > **7k** > **7a** > **7b** > **7l** > **7d** (Tables 1–3).

The isoform *h*CA II, being linked with glaucoma, was strongly inhibited by all the newly synthesized ketene *N*,*S*-acetal sulfonamides, **7a–o**, with IC_{50} and K_I values spanning in the low nanomolar range (IC_{50} ranging from 8.44 ± 0.06 to 19.88 ± 0.27 nM and K_I ranging from 7.41 ± 0.03 to 56.75 ± 0.20 nM). These 15 analogs (**7a–o**) indicated a better inhibition capacity than standard drug AAZ (K_I 97.73 ± 1.62 nM). Compound **7o** (2-[2,2-dicyano-1-(4-iodophenylamino)vinylthio]-*N*-(4-sulfamoylphenyl)acetamide) containing 4-iodine (K_I 7.41 ± 0.03 nM) was found to have the most potent inhibition profile, whereas derivative **7m** containing 4-fluorine (K_I 56.75 ± 0.20 nM) was found to have the weakest inhibition profile against physiological isoform *h*CA II. The comparison of inhibitory activity of these sulfonamides (**7o** and **7m**) revealed that the replacement of the 4-iodine of compound **7o** by a fluorine group of analog **7m** caused an approximately 7.5-fold reduction in the inhibition. On the contrary, the displacement of the fluorine

from position 4 to position 3 repristinated the inhibition (compound **7l**, K_I 17.84 ± 0.12 nM). As a general trend, the replacement of the 4-iodine atom of compound **7o** by other groups, such as methyl (**7b**, K_I 10.53 ± 0.17 nM), nitro (**7e**, K_I 19.46 ± 0.16 nM), bromine (**7h**, K_I 54.65 ± 0.87 nM), chlorine (**7i**, K_I 32.35 ± 0.67 nM), and fluorine (**7m**, K_I 56.75 ± 0.20 nM), led to a decline in the inhibition. However, the presence of two chlorine atoms (compounds **7j** and **7k**, K_Is 24.60 ± 0.31 and 16.09 ± 0.06 nM, respectively) caused a reduction in inhibition when compared with **7o** analog. The replacement of the 4-iodine of compound **7o** by a 2-methoxy group (**7c**, K_I 13.07 ± 0.19 nM) reduced the inhibition level by 2-fold; also, the replacement by a 2-bromine atom (**7f**, K_I 33.58 ± 0.62 nM) contributed an approximately 4.5-fold reduction in inhibition. In general, it was found that the ketene *N*,*S*-acetal sulfonamides having the functional groups of substituents on the aryl ring were found to be potent inhibitors of isoform *h*CA II. Concerning the effect of substitution of the phenylamino moiety (**7a–o**), the *h*CA II inhibitory activities were reduced in the following order: **7o** > **7b** > **7g** > **7c** > **7k** > **7d** > **7l** > **7e** > **7a** > **7j** > **7i** > **7f** > **7n** > **7h** > **7m**. Interestingly, the analogs bearing methoxy and nitro groups (**7c** and **7e**, S_Is 3.69 and, 5.44, respectively) on the aryl ring exhibited the highest selectivity index for *h*CA I, whereas the derivatives containing fluorine and trifluoromethyl moiety (**7m** and **7n**, S_Is 2.65 and 2.23, respectively) displayed a remarkable selectivity profile for *h*CA II, compared with the other substituents in this study (Tables 1–3).

All of the synthesized new series of ketene *N*,*S*-acetal sulfonamides (**7a–o**) displayed a good inhibitory activity against AChE enzyme (linked with AD), with IC_{50} values ranging between 6.81 ± 0.11 and 24.37 ± 0.38 nM and K_I constants ranging from 7.37 ± 0.31 to 32.89 ± 5.14 nM. Here, analog **7i** (2-[1-(4-chlorophenylamino)-2,2-dicyanovinylthio]-*N*-(4-sulfamoylphenyl)acetamide) containing 4-chlorine exhibited the highest inhibition with K_I constant of 7.37 ± 0.31 nM, almost 21-fold stronger than the standard drug (TAC, K_I 159.64 ± 0.87 nM). Herein, the different substituents on the aryl ring (**7a–o**) played a crucial role in the AChE inhibition activity. The replacement of chlorine by bromine, fluorine, and iodine at the same position of aryl ring decreased enzyme inhibition in such a manner that K_I constants for compounds **7h**, **7m**, and **7o** have the following values: 15.07 ± 0.35, 15.23 ± 0.60, and 32.89 ± 5.14 nM, respectively. However, the presence of bromine at position 2 (**7f**, K_I 10.84 ± 0.16 nM) increased antienzyme activity than 4-substituted compound **7h**. Compound **7n** possessing 3-trifluoromethyl moiety also exhibited a high inhibition activity (K_I 11.16 ± 0.54 nM). Also, compounds **7j** and **7k** possessing two Cl groups at 2-, 4- and 3-, 5-positions of aryl ring showed a lower inhibition profile than analog **7i** (**7j** and **7k**, K_Is 12.23 ± 0.93 and 18.94 ± 1.50 nM, respectively). Furthermore, derivatives **7b** and **7e** possessing methyl and nitro groups at position 3 displayed a moderate similar activity (K_Is 22.62 ± 1.07 and 22.14 ± 2.47 nM, respectively). Interestingly, the transposal of the 2-methoxy group from the aryl ring of compound **7c** to position 3 to give isomeric **7d** led to about a twofold decrease in the inhibition activity (K_Is 12.70 ± 0.66 and 23.68 ± 1.56 nM, respectively). Out of the newly synthesized ketene *N*,*S*-acetal sulfonamide derivatives (**7a–o**), the compounds **7i**, **7f**, and **7n** containing 4-fluorine, 2-bromine, and 3-trifluoromethyl groups were found to be the most effective AChE inhibitors amongst their respective groups of derivatives. In this respect, the order of the compound inhibitory strength of K_I constants is as follows: **7i** > **7f** > **7n** > **7j** > **7c** > **7h** > **7m** > **7g** > **7k** > **7e** > **7a** > **7b** > **7d** > **7l** > **7o** (Tables 1–3).

2.3 | In silico studies

2.3.1 | ADMET study

The ADMET properties (adsorption, distribution, metabolism, excretion, and toxicity) and some pharmacokinetic parameters of the new synthesized ketene *N*,*S*-acetal sulfonamide derivatives (**7a–o**) were estimated by using the QikProp module in Maestro. The overall predicted values are summarized in Table 4. The molecular weights (MWs 413.47–539.37), total solvent-accessible surface areas (SASAs 666.60–752.60), and total solvent-accessible volumes (1,196.43–1,208.88) of the compounds (**7a–o**) have been determined to be in the permissible values. The logP values (QPlogPw and QPlogPo/w), which indicate the hydrophilicity/lipophilicity of the analogs (**7a–o**), are in the acceptable range. All the compounds (**7a–o**) have displayed good skin permeability ranges (QPlogKps ranging from −4.43 to −6.81) and the van der Waals surface area values (PSAs ranging between 135.74 and 199.67). QPlogS, which is an aqueous solubility descriptor, was found in the permissible values, compared with standard ranges. Brain/blood partition coefficient (QPlogBB) values range from −2.73 to −3.87, which indicates that these compounds (**7a–o**) have a moderate capability. Human serum albumin-binding coefficient (QPlogKhsa ranging from −0.32 to −0.68) values and IC_{50} value for the blockage of HERG K^+ channels (QPlogHERG ranging from −5.34 to −6.76) values are in the acceptable range (−1.5 to 1.5 and less than −5, respectively) for these target derivatives (**7a–o**). The estimated values of human oral absorption (HOA) are between 16.70% and 64.97%, indicating that all compounds (**7a–o**, except **7e**) are in an acceptable range. In summary, the ADMET results revealed that the synthesized active analogs (**7a–o**) possess the drug-likeness criteria conformed by both Jorgensen's rule of three[55] and Lipinski's rule of five.[56] These compounds can be regarded as promising lead compounds for designing more potent *h*CA I, II, and AChE inhibitors that may be novel drug candidates.

2.3.2 | Molecular docking study

To describe the trends determined for the observed relative potency and selectivity of our designed and synthesized new compounds (**7a–o**), docking and molecular mechanics–generalized Born surface area (MM–GBSA)-based refinements studies were performed for the selected analogs as representative of the derivatives. Before molecular docking, key residues in the active sites and the noncovalent contacts between the receptor–ligand complexes were investigated

TABLE 4 ADMET-related parameters of the compounds (**7a–o**)

Principal descriptors	7a	7b	7c	7d	7e	7f	7g	7h	7i	7j	7k	7l	7m	7n	7o	Standard range
QPlogPw	20.48	19.43	20.68	20.67	21.08	19.90	19.73	19.54	18.42	20.04	19.40	19.70	20.23	19.61	19.61	4 to 45
QPlogPo/w	0.23	0.33	0.36	0.35	−0.36	0.60	0.82	0.72	1.79	1.22	1.19	0.48	0.47	1.23	0.85	−2.0 to 6.5
QPlogS	−4.75	−4.24	−4.87	−4.94	−4.50	−4.99	−5.00	−4.81	−5.99	−6.01	−5.49	−4.57	−5.06	−5.41	−5.02	−6.5 to 1.5
QPlogKp	−5.31	−5.56	−5.33	−5.32	−6.81	−5.44	−5.10	−5.33	−4.43	−5.45	−5.31	−5.15	−5.42	−5.07	−5.20	−8.0 to −1.0
QPlogBB	−3.56	−3.03	−3.61	−3.64	−3.87	−2.79	−2.85	−2.86	−2.46	−2.70	−2.75	−2.94	−3.43	−2.73	−2.87	−3.0 to 1.2
QPlogKhsa	−0.62	−0.51	−0.61	−0.62	−0.68	−0.56	−0.53	−0.53	−0.32	−0.42	−0.46	−0.60	−0.59	−0.44	−0.52	−1.5 to 1.5
QPlogHERG	−6.76	−5.34	−6.55	−6.62	−6.09	−5.59	−6.15	−6.04	−6.64	−6.46	−6.55	−5.79	−6.68	−6.58	−5.95	<−5
HOA	44.81	47.32	46.20	46.36	16.70	48.31	52.94	51.15	64.97	51.91	54.96	50.35	46.45	56.23	39.76	<25 poor, great >500
PSA	161.43	157.01	168.23	170.05	199.67	159.60	156.40	154.99	135.74	159.65	154.75	156.23	161.42	154.68	154.61	7 to 200
Rule of Five	0	0	0	0	1	0	0	0	0	0	0	0	0	0	1	max. 4
Rule of Three	1	1	1	1	1	1	1	1	1	2	1	1	1	1	1	max. 3

Note: Various computational pharmacodynamic and pharmacokinetic parameters of synthesized compounds were predicted in this study, such as water/gas partition coefficient (QPlogPw), octanol/water partition coefficient (QPlogPo/w), aqueous solubility (QPlogS), skin permeability (QPlogKp), brain/blood partition coefficient (QPlogBB), human serum albumin-binding (QPlogKhsa), IC_{50} value for blockage of HERG K^+ channels (QPlogHERG), human oral absorption (HOA), the van der Waals surface area of polar nitrogen and oxygen atoms (PSA), the number of violations of Lipinski's rule of five, and the number of violations of Jorgensen's rule of three.

Abbreviation: ADMET, adsorption, distribution, metabolism, excretion, and toxicity.

by the Protein Contacts Atlas (http://www.mrc-lmb.cam.ac.uk/pca). The X-ray crystal structures of 5E2M (for *h*CA I) and 4M0E (for AChE) were present in the form of a homodimer chain; hence, their chain A was chosen for in silico studies. V14 (PubChem CID 73774785, $C_{16}H_{23}F_3N_2O_5S_2$, 3-(cyclooctylamino)-2,5,6-trifluoro-4-[(2-hydroxyethyl)sulfonyl]benzenesulfonamide), FK8 (PubChem CID 12136, $C_8H_9NO_2$, benzylcarbamate), and 1YL (PubChem CID 11425923, $C_{18}H_{14}O_3$, (1*R*)-1,6-dimethyl-1,2-dihydronaphtho[1,2-*g*][1]benzofuran-10,11-dione) were the cocrystallized ligands with 5E2M, 6H29, and 4M0E, respectively. The molecular docking protocol for these proteins was validated by extracting the bound ligands (V14, FK8, and 1YL) from the receptors and again redocking them on the same sites.[57] The docking poses were superimposed, and root-mean-square deviation values were computed to be 1.14, 0.99, and 0.10 Å, respectively. The most active compounds (**7a–o**), against *h*CA I, *h*CA II, and AChE, were docked into the binding sites of the receptors complexed with the V14 (PDB iD 5E2M), FK8 (PDB iD 6H29), and 1YL (PDB iD 4M0E).

According to the literature, the native ligand (V14) displays three major interactions, like H-bond interaction with His67, Thr199, and Pro201, π–π stacking with His67, and His94 and a salt bridge between Leu198 and the Zinc ion, and the docking score was −10.12 in the catalytic domain of 5E2M. For the most active compound (**7g**, K_I 9.01 ± 0.08 nM), the docking score (−5.81) was found low for the cocrystallized ligand. Compound **7g** exhibited H-bond interactions with Trp5, Val62, His64, His67, and Pro201. It also displayed π–π stacking with His64 and His 200, and it made both π–cation interaction and salt bridge with Zn metal (Figure 1). But according to the docking scores, derivative **7f** displayed the best docking score (−7.90) among the analogs. Compound **7f** made H-bond with Trp5, His64, Gln92, and Pro201. It also showed π–π stacking with His64, Phe91, and His 200.

The 6H29 complexed with FK8 shows two H-bonds with Asn67. Apart from this, FK8 showed hydrophobic interactions with Ala65, Val121, Leu141, Val143, Leu198, Val207, and Trp209. The docking score was −4.40, which was surprisingly low, as it was expected to range between −5.00 and −6.00. It may be possible that interaction with Zinc ion was not monitored in the docked pose, so the docking score might be lower. Compound **7o**, which is the most inhibitory activity compound (K_I 7.41 ± 0.03), revealed interaction modes between the 6H29 and ligands, which further deepened the understanding of SAR. As shown in Figure 2, compound **7o** formed H-bonds with the active site residues; for example, the carbonyl group of the acetamide skeleton as H-bond acceptor formed an H-bond with Gln92, the aromatic portion of the benzenesulfonamide core exhibited π–π stacking with His94, and also the oxygen atom of the sulfonamide formed metal coordination with the zinc metal, as reported by Ahmed et al.[58] However, based on the dock score, compound **7e** exhibited the best docking score (−5.82) among the 15 derivatives used for this investigation. Compound **7e** formed four H-bonds with the active site residues, that is, the amino moiety of the sulfonamide skeleton as H-bond donor formed two H-bonds with Phe70 and Asp72, the nitrogen atoms at position 2 of the thioacetamide skeleton as H-bond acceptor formed two hydrogen bonds with Asn62 and Gln92.

In fact, a first look at the active sites of *h*CA I and *h*CA II, we can obtain some useful information. The main difference among the isoforms is the size of the active sites. The smaller binding site of *h*CA I can explain the lower activity of the compound **7o** on this isoform. Second prominent data, the structural difference between *h*CA I and the *h*CA II is residues, which is His64 in *h*CA I, whereas Gly92 in *h*CA II. As in most of the poses of the docked analogs used in this study, there is an interaction between the ligand and His64, and the Gly/His residues probably lead to the ligands' higher activity toward *h*CA I.

1YL, which is previously reported as the native ligand, and analog **7i** (K_I 7.37 ± 0.31 nM), which is the most active analog of the series, were analyzed in terms of interactions with AChE. Unsurprisingly, the docking modes into 4M0E determined for the two ligands were very similar to that estimated for their other analogs, as both 1YL and compound **7i** displayed the same interactions with Trp286, and the docking scores were −10.36 and −7.42, respectively. Within 4M0E active site, the chlorine atom on the aryl ring and the amino moiety of the benzenesulfonamide group of compound **7i** showed potential two H-bonds with Tyr133 and Ser293, respectively, whereas 1YL established an H-bond by the carbonyl group with Phe295. A hydrophobic interaction was monitored between derivative **7i** and Tyr72, Trp86, Tyr124, Leu289, Val294, Phe295, Phe297, Tyr337, Phe338, Tyr341, and Ile451. Apart from these, derivative **7i** also exhibited a polar interaction with Asn87 and Ser125. The docking score of compound **7n** was −9.74, which was better than compound **7i** because compound **7n** formed more interactions with residues and also formed an H-bond with Ser293 (Figure 3).

Furthermore, Prime MM–GBSA (ΔG Bind) ranges were found as −15.40 and −47.43 kcal/mol (compounds **7h** and **7f**) for 5E2M, −13.45 and −35.29 kcal/mol (analogs **7k** and **7b**) for 6H29, and −7.86 and −65.44 kcal/mol (derivatives **7i** and **7g**) for 4M0E. Among the analogs, **7f** (with 5E2M), **7b** (with 6H29), and **7g** (with 4M0E) were determined to exhibit more binding-free energy, −47.43, −35.29, and −65.44 kcal/mol, respectively; hence, they are more effective than other compounds.

3 | CONCLUSION

In summary, this study reports the design, synthesis, and characterization of 15 new ketene *N,S*-acetal benzenesulfonamides and their evaluation as inhibitors of *h*CA isoforms I, II, and AChE. In general, all the synthesized derivatives inhibited *h*CA I, II, and AChE, which were found in the low nanomolar range. Furthermore, all analogs showed a better inhibition profile than the standard drugs AAZ and TAC for *h*CA isoforms and AChE. Compounds **7c** and **7e** selectively inhibited edema-associated isoform *h*CA I, whereas derivatives **7m** and **7n** selectively inhibited edema, epilepsy, and glaucoma-linked isoform *h*CA II. It is further found that halogen-appended analogs, **7g** (for *h*CA I), **7o** (for *h*CA II), and **7i** (for AChE), are stronger inhibitors of tested enzymes as compared to their

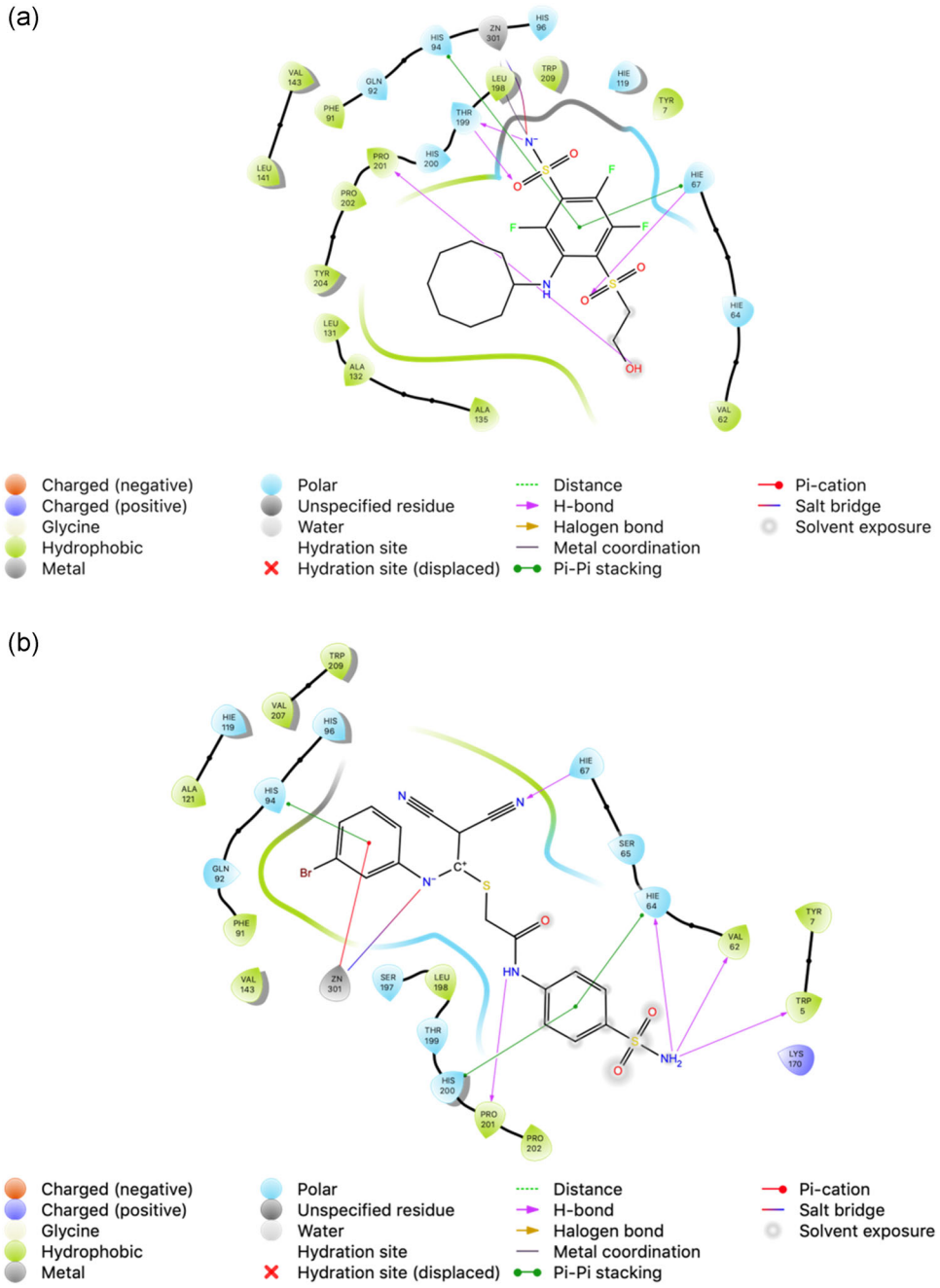

FIGURE 1 Interaction of the ligands with the key amino acids within the binding site of *h*CA I (human carbonic anhydrase; PDB ID 5E2M). (a) Docking pose of the native ligand V14 (3-(cyclooctylamino)-2,5,6-trifluoro-4-[(2-hydroxyethyl)sulfonyl]benzenesulfonamide). (b) Docking pose of compound **7g** (2-[1-(3-bromophenylamino)-2,2-dicyanovinylthio]-*N*-(4-sulfamoylphenyl)acetamide)

corresponding parent 2-[2,2-dicyano-1-(phenylamino)vinylthio]-*N*-(4-sulfamoylphenyl)acetamide derivatives **7a**–**o**. In this context, molecular docking and MM–GBSA studies of compounds **7g**, **7o**, and **7i** in the binding sites of *h*CA I, II, and AChE provide insights into the details of the binding interactions producing the inhibition profiles. Also, the SAR study helped us gain an understanding of the relationship between structure and activity. So, it may be concluded that these shreds of evidence may prove precious in the design and synthesis of more selective and more effective CA and AChE inhibitors.

4 | EXPERIMENTAL

4.1 | Chemistry

4.1.1 | General

All starting materials and reagents were commercially available and used without further purification except where indicated. Melting points were determined on a Yanagimoto micro-melting point

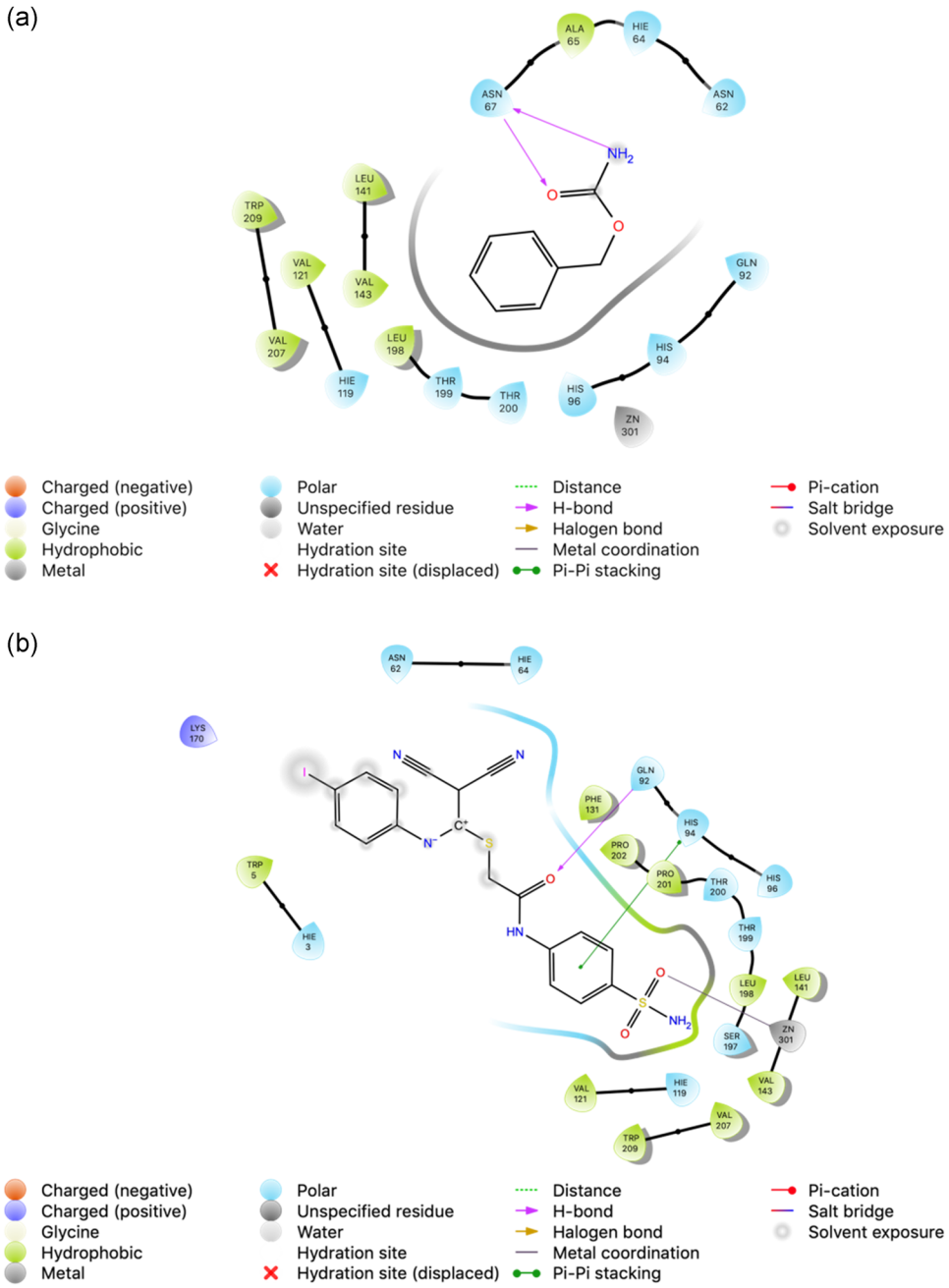

FIGURE 2 Interaction of the ligands with the key amino acids within the binding site of *h*CA II (human carbonic anhydrase; PDB ID 6H29). (a) Docking pose of the native ligand FK8 (benzylcarbamate). (b) Docking pose of compound **7o** (2-[2,2-dicyano-1-(4-iodophenylamino) vinylthio]-*N*-(4-sulfamoylphenyl)acetamide)

apparatus and were uncorrected. Infrared (IR) spectra were measured on a Shimadzu Prestige-21 (200 VCE) spectrometer. ^{1}H and ^{13}C NMR spectra were recorded on a Varian Infinity Plus 300 spectrometer at 75 MHz. ^{1}H and ^{13}C chemical shifts are referenced to the internal deuterated solvent. Chemical shift values (δ) are given in ppm. The elemental analysis was carried out with a Leco CHNS-932 instrument. All chemicals were purchased from Merck and Sigma-Aldrich.

The InChI keys of the investigated compounds are provided as Supporting Information.

4.1.2 | Synthesis of acetylchloride-substituted sulfonamide 3

A solution of sulfanilamide (**1**) (2 mmol) in DMF (5 ml) and TEA (2 mmol) was cooled down to 0°C, and then acetylchloride (**2**) (3 mmol) was added dropwise while stirring. The whole reaction was maintained at 0°C in an ice bath for 5 hr and then poured into a beaker containing ice/water mixture with a few drops of hydrochloric acid. The solid product was washed with water and collected by filtration, dried, and crystallized from ethanol.

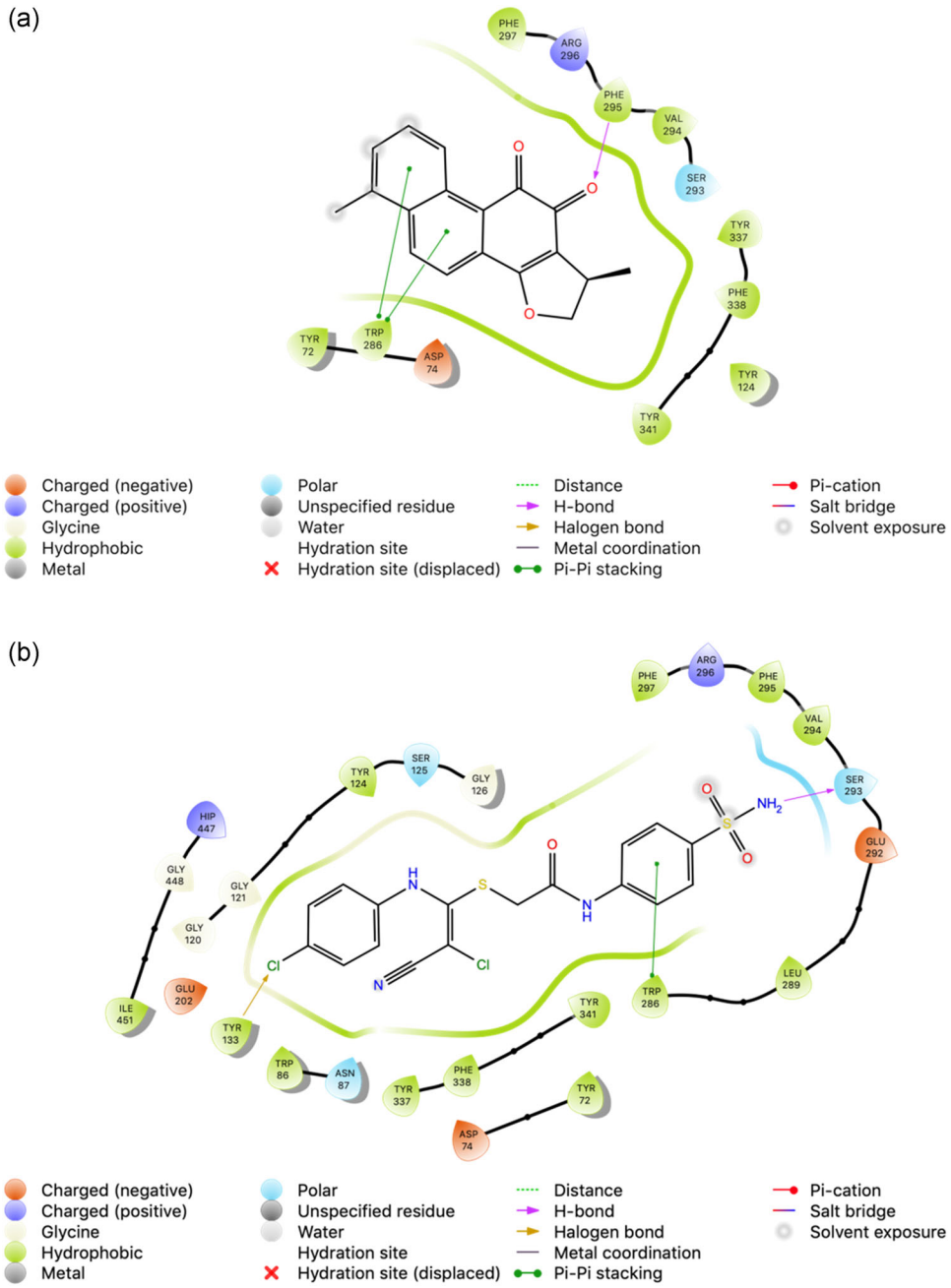

FIGURE 3 Interaction of the ligands with the key amino acids within the binding site of AChE (acetylcholinesterase; PDB ID 4M0E). (a) Docking pose of the native ligand 1YL ((1*R*)-1,6-dimethyl-1,2-dihydronaphtho[1,2-*g*][1]benzofuran-10,11-dione)). (b) Docking pose of compound **7i** (2-[1-(4-chlorophenylamino)-2,2-dicyanovinylthio]-*N*-(4-sulfamoylphenyl)acetamide)

4.1.3 | General procedure for the synthesis of compound 6

A solution of isocyanate compound **4** (2 mmol) in DMF (5 ml) was mixed at room temperature and then malononitrile (2 mmol) and potassium hydroxide (1.3 mmol) were added while stirring. The whole reaction mixture was mixed at room temperature overnight.

4.1.4 | General procedure for the synthesis of ketene *N,S*-acetal-substituted sulfonamide compounds 7a–o

Compound **3** (2 mmol) was added to compound **6** (2 mmol) and was stirred overnight at room temperature. Ice-cold water was added into the reaction mixture with a few drops of hydrochloric

acid. The solid product formed was washed with water and collected by filtration, dried, and crystallized from hexane/acetone.

*2-[2,2-Dicyano-1-(phenylamino)vinylthio)]-N-(4-sulfamoylphenyl)-acetamide (**7a**)*

Yield 86.6%, m.p. 200°C; IR (cm^{-1}): 3,349 ($-NH_2$), 3,202 (–NH), 3,133 (=C–H, aromatic), 2,988 ($-CH_2$, aliphatic), 2,207 (CN), 1,660 (C=O), 1,621 (C=C), 1,320, and 1,152 (S=O; Figure S1); ^{1}H NMR (300 MHz, dimethyl sulfoxide [DMSO]-d_6, ppm): 10.6–10.8 (2H, s, –NH), 7.76 (2H, d, =CH, *J* = 8.6 Hz), 7.68 (2H, d, =CH, *J* = 8.7 Hz), 7.2–7.5 (5H, m, =CH), 7.30 (2H, s, –NH2), and 4.1 (2H, s, $-CH_2$; Figure S2); ^{13}C NMR (75 MHz, DMSO-d_6, ppm): 169.9, 166.6, 141.9, 139.6, 138.9, 129.9, 127.5, 127.3, 124.2, 119.6, 117, 114.3, and 38 (Figure S3). Anal. calcd. for $C_{18}H_{15}N_5O_3S_2$: C, 52.29; H, 3.66; N, 16.94; O, 11.61; S, 15.51. Found: C, 52.35; H, 3.76; N, 16.99; O, 11.70; S, 15.56.

*2-[1-(p-Toluidino)-2,2-dicyanovinylthio]-N-(4-sulfamoylphenyl)-acetamide (**7b**)*

Yield 66.5%, m.p. 206°C; IR (cm^{-1}): 3,305 ($-NH_2$), 3,203 (–NH), 3,133 (=C–H, aromatic), 2,988 ($-CH_2$, aliphatic), 2,220 (CN), 1,665 (C=O), 1,626 (C=C), 1,320, and 1,153 (S=O; Figure S4); ^{1}H NMR (300 MHz, DMSO-d_6, ppm): 10.6–10.8 (2H, s, –NH), 7.77 (2H, d, =CH, *J* = 8.6 Hz), 7.69 (2H, d, =CH, *J* = 8.7 Hz), 7.0 (2H, d, =CH, *J* = 8.4 Hz), 7.42 (2H, d, =CH, *J* = 8.3 Hz), 7.30 (2H, s, $-NH_2$), 4.1 (2H, s, $-CH_2$), and 2.3 (3H, s, $-CH_3$; Figure S5); ^{13}C NMR (75 MHz, DMSO-d_6, ppm): 170.1, 166.6, 141.9, 139.54, 136.6, 136.4, 130.3, 127.5, 127.4, 124.1, 123.3, 119.6, 37.9, and 21.3 (Figure S6). Anal. calcd. for $C_{19}H_{17}N_5O_3S_2$: C, 52.38; H, 4.01; N, 16.38; O, 11.23; S, 15.00. Found: C, 52.45; H, 4.11; N, 16.44; O, 11.29; S, 15.08.

*2-[2,2-Dicyano-1-(2-methoxyphenylamino)vinylthio]-N-(4-sulfamoylphenyl)acetamide (**7c**)*

Yield 69.2%, m.p. 217°C; IR (cm^{-1}): 3,308 ($-NH_2$), 3,205 (–NH), 3,133 (=C–H, aromatic), 2,981 ($-CH_2$, aliphatic), 2,214 (CN), 1,670 (C=O), 1,622 (C=C), 1,343, and 1,155 (S=O; Figure S7); ^{1}H NMR (300 MHz, DMSO-d_6, ppm): 10.5–10.7 (2H, s, –NH), 7.77 (2H, d, =CH, *J* = 8.9 Hz), 7.72 (2H, d, =CH, *J* = 8.8 Hz), 6.9–7.4 (4H, m, =CH), 7.30 (2H, s, $-NH_2$), 4.2 (2H, s, $-CH_2$), and 3.8 (3H, s, $-CH_3$; Figure S8); ^{13}C NMR (75 MHz, DMSO-d_6, ppm): 169.8, 166.6, 160.4, 142.3, 140.7, 130.3, 127.5, 126.15, 119.6, 117, 116.3, 114.3, 113.2, 109.7, 55.3, and 37.95 (Figure S9). Anal. calcd. for $C_{19}H_{17}N_5O_4S_2$: C, 51.46; H, 3.86; N, 15.79; O, 14.43; S, 14.46. Found: C, 51.49; H, 3.89; N, 15.84; O, 14,49; S, 14.51.

*2-[2,2-Dicyano-1-(3-methoxyphenylamino)vinylthio]-N-(4-sulfamoylphenyl)acetamide (**7d**)*

Yield 73.5%, m.p. 210°C; IR (cm^{-1}): 3,265 ($-NH_2$), 3,202 (–NH), 3,077 (=C–H, aromatic), 2,988 ($-CH_2$, aliphatic), 2,217 (CN), 1,660 (C=O), 1,615 (C=C), 1,319, and 1,149 (S=O; Figure S10); ^{1}H NMR (300 MHz, DMSO-d_6, ppm): 10.6–10.8 (2H, s, –NH), 7.76 (2H, d, =CH, *J* = 8.6 Hz), 7.70 (2H, d, =CH, *J* = 8.6 Hz), 7.30 (2H, s, $-NH_2$), 6.8–7.3 (4H, m, =CH), 4.1 (2H, s, $-CH_2$), and 3.7 (3H, s, $-CH_3$; Figure S11); ^{13}C NMR (75 MHz, DMSO-d_6, ppm): 169.8, 166.6, 160.3, 141.9, 140, 139.54, 130.7, 128, 127.5, 119.6, 117, 114.3, 113.2, 109.7, 55.9, and 38 (Figure S12). Anal. calcd. for $C_{19}H_{17}N_5O_4S_2$: C, 51.46; H, 3.86; N, 15.79; O, 14.43; S, 14.46. Found: C, 51.52; H, 3.89; N, 15.85; O, 14.49; S, 14.48.

*2-[2,2-Dicyano-1-(4-nitrophenylamino)vinylthio]-N-(4-sulfamoylphenyl)acetamide (**7e**)*

Yield 86.5%, m.p. 215°C; IR (cm^{-1}): 3,300 ($-NH_2$), 3,200 (–NH), 3,077 (=C–H, aromatic), 2,948, ($-CH_2$, aliphatic), 2,225 (CN), 1,653 (C=O), 1,614 (C=C), 1,496 (NO_2), 1,309, and 1,151 (S=O; Figure S13); ^{1}H NMR (300 MHz, DMSO-d_6, ppm): 10.6–11.2 (2H, s, –NH), 7.74 (2H, d, =CH, *J* = 8.7 Hz), 7.65 (2H, d, =CH, *J* = 8.8 Hz), 7.42 (2H, d, =CH, *J* = 8.4 Hz), 7.40 (2H, d, =CH, *J* = 8.3 Hz), 7.20 (2H, s, $-NH_2$), and 4.1 (2H, s, $-CH_2$; Figure S14); ^{13}C NMR (75 MHz, DMSO-d_6, ppm): 166.4, 152.5, 149.5, 141.8, 139.58, 131.9, 128, 127.5, 125.7, 125.5, 122.98, 119.6, and 39.3 (Figure S15). Anal. calcd. for $C_{18}H_{14}N_6O_5S_2$: C, 47.16; H, 3.08; N, 18.33; O, 17.45; S, 13.99. Found: C, 47.19; H, 3.12; N, 18.39; O, 17.48; S, 14.05.

*2-[1-(2-Bromophenylamino)-2,2-dicyanovinylthio]-N-(4-sulfamoylphenyl)acetamide (**7f**)*

Yield 76.7%, m.p. 205°C; IR (cm^{-1}): 3,405 ($-NH_2$), 3,200 (–NH), 3,127 (=C–H, aromatic), 2,984, ($-CH_2$, aliphatic), 2,220 (CN), 1,665 (C=O), 1,600 (C=C), 1,334, and 1,162 (S=O; Figure S16); ^{1}H NMR (300 MHz, DMSO-d_6, ppm): 10.6–10.8 (2H, s, –NH), 7.81 (2H, d, =CH, *J* = 8.6 Hz), 7.76 (2H, d, =CH, *J* = 8.7 Hz), 7.2–7.6 (4H, m, =CH), 7.20 (2H, s, $-NH_2$), and 4.1 (2H, s, $-CH_2$; Figure S17); ^{13}C NMR (75 MHz, DMSO-d_6, ppm): 170.8, 167.1, 141.8, 139.7, 137.5, 134.2, 133.8, 130.2, 129.9, 128.8, 128.5, 125.7, 127.5, 121.98, 119.6, and 38.2 (Figure S18). Anal. calcd. for $C_{18}H_{14}BrN_5O_3S_2$: C, 43.91; H, 2.87; Br, 16.23; N, 14.22; O, 9.75; S, 13.02. Found: C, 43.98; H, 2.89; Br, 16.27; N, 14.26; O, 9.79; S, 13.12.

*2-[1-(3-Bromophenylamino)-2,2-dicyanovinylthio]-N-(4-sulfamoylphenyl)acetamide (**7g**)*

Yield 73.7%, m.p. 215°C; IR (cm^{-1}): 3,361 ($-NH_2$), 3,271 (–NH), 3,118 (=C–H, aromatic), 2,988, ($-CH_2$, aliphatic), 2,213 (CN), 1,705 (C=O), 1,658 (C=C), 1,326, and 1,153 (S=O; Figure S19); ^{1}H NMR (300 MHz, DMSO-d_6, ppm): 10.6–10.8 (2H, s, –NH), 7.78 (2H, d, =CH, *J* = 8.9 Hz), 7.70 (2H, d, =CH, *J* = 8.7 Hz), 7.2–7.6 (4H, m, =CH), 7.20 (2H, s, $-NH_2$), and 4.1 (2H, s, $-CH_2$; Figure S20); ^{13}C NMR (75 MHz, DMSO-d_6, ppm): 170.2, 166.6, 141.9, 140.6, 139.62, 131.8, 129.8, 127.5, 127.4, 126.4, 125.5, 122.9, 122.4, 119.6, and 38.4 (Figure S21). Anal. calcd. for $C_{18}H_{14}BrN_5O_3S_2$: C, 43.91; H, 2.87; Br, 16.23; N, 14.22; O, 9.75; S, 13.02. Found: C, 43.98; H, 2.89; Br, 16.28; N, 14.27; O, 9.79; S, 13.09.

*2-[1-(4-Bromophenylamino)-2,2-dicyanovinylthio]-N-(4-sulfamoylphenyl)acetamide (**7h**)*

Yield 77.7%, m.p. 190°C; IR (cm^{-1}): 3,305 ($-NH_2$), 3,211 (–NH), 3,139 (=C–H, aromatic), 2,988, ($-CH_2$, aliphatic), 2,221 (CN), 1,660 (C=O), 1,628 (C=C), 1,314, and 1,151 (S=O; Figure S22); ^{1}H NMR (300 MHz, DMSO-d_6, ppm): 10.6–10.8 (2H, s, –NH), 7.76 (2H, d, =CH,

J = 8.6 Hz), 7.68 (2H, d, =CH, *J* = 8.8 Hz), 7.58 (2H, d, =CH, *J* = 7.8 Hz), 7.31 (2H, d, =CH, *J* = 7.9 Hz), 7.20 (2H, s, $-NH_2$), and 4.1 (2H, s, $-CH_2$; Figure S23); ^{13}C NMR (75 MHz, DMSO-d_6, ppm): 170.2, 166.6, 141.9, 139.62, 138.4, 133.3, 132.8, 132, 127.5, 125.9, 119.6, 119.5, and 38.3 (Figure S24). Anal. calcd. for $C_{18}H_{14}BrN_5O_3S_2$: C, 43.91; H, 2.87; Br, 16.23; N, 14.22; O, 9.75; S, 13.02. Found: C, 43.95; H, 2.89; Br, 16.28; N, 14.29; O, 9.79; S, 13.10.

2-[1-(4-Chlorophenylamino)-2,2-dicyanovinylthio]-N-*(4-sulfamoylphenyl)acetamide (**7i**)*

Yield 79.9%, m.p. 188°C; IR (cm^{-1}): 3,260 ($-NH_2$), 3,202 (–NH), 3,143 (=C–H, aromatic), 2,805 ($-CH_2$, aliphatic), 2,220 (CN), 1,660 (C=O), 1,628 (C=C), 1,319, and 1,152 (S=O; Figure S25); ^{1}H NMR (300 MHz, DMSO-d_6, ppm): 10.6–10.8 (2H, s, –NH), 7.76 (2H, d, =CH, *J* = 8.6 Hz), 7.68 (2H, d, =CH, *J* = 8.7 Hz), 7.32 (2H, d, =CH, *J* = 8.1 Hz), 7.28 (2H, d, =CH, *J* = 8.1 Hz), 7.20 (2H, s, $-NH_2$), and 4.1 (2H, s, $-CH_2$; Figure S26); ^{13}C NMR (75 MHz, DMSO-d_6, ppm): 170.2, 166.5, 141.9, 139.62, 138, 131.2, 129.9, 129.8, 127.5, 127.4, 125.5, 119.6, and 38.3 (Figure S27). Anal. calcd. for $C_{18}H_{14}ClN_5O_3S_2$: C, 48.27; H, 3.15; Cl, 7.92; N, 15.64; O, 10.72; S, 14.32. Found: C, 48.31; H, 3.19; Cl, 7.98; N, 15.69; O, 10.75; S, 14.36.

2-[2,2-Dicyano-1-(2,4-dichlorophenylamino)vinylthio]-N-*(4-sulfamoylphenyl)acetamide (**7j**)*

Yield 79.9%, m.p. 207°C; IR (cm^{-1}): 3,308 ($-NH_2$), 3,211 (–NH), 3,071 (=C–H, aromatic), 2,957 ($-CH_2$, aliphatic), 2,222 (CN), 1,662 (C=O), 1,621 (C=C), 1,331, and 1,149 (S=O; Figure S28); ^{1}H NMR (300 MHz, DMSO-d_6, ppm): 10.6–10.8 (2H, s, –NH), 7.77 (2H, d, =CH, *J* = 8.8 Hz), 7.73 (2H, d, =CH, *J* = 8.8 Hz), 7.4 (3H, m, =CH), 7.20 (2H, s, $-NH_2$), and 4.1 (2H, s, $-CH_2$; Figure S29); ^{13}C NMR (75 MHz, DMSO-d_6, ppm): 167.6, 141.8, 139.9, 133.4, 131.4, 130.2, 130.1, 129.6, 129.1 127.5, 127.4, 119.7, 119.6, and 38.2 (Figure S30). Anal. calcd. for $C_{18}H_{13}Cl_2N_5O_3S_2$: C, 44.82; H, 2.72; Cl, 14.70; N, 14.52; O, 9.95; S, 13.29. Found: C, 44.88; H, 2.77; Cl, 14.74; N, 14.56; O, 9.99; S, 13.34.

2-[2,2-Dicyano-1-(3,5-dichlorophenylamino)vinylthio]-N-*(4-sulfamoylphenyl)acetamide (**7k**)*

Yield 70.9%, m.p. 235°C; IR (cm^{-1}): 3,275 ($-NH_2$), 3,214 (–NH), 3,086 (=C–H, aromatic), 2,989 ($-CH_2$, aliphatic), 2,216 (CN), 1,662 (C=O), 1,621 (C=C), 1,317, and 1,160 (S=O; Figure S31); ^{1}H NMR (300 MHz, DMSO-d_6, ppm): 10.6–10.8 (2H, s, –NH), 7.76 (2H, d, =CH, *J* = 8.4 Hz), 7.67 (2H, d, =CH, *J* = 8.4 Hz), 7.2–7.6 (3H, =CH), 7.4 (2H, s, $-NH_2$), 4.1 (2H, s, $-CH_2$; Figure S32); ^{13}C NMR (75 MHz, DMSO-d_6, ppm): 170.5, 166.06, 141.8, 139.64, 135.3, 135.1, 131.7, 129.1, 128.1, 127.5, 126.2, 122.3, 119.6, 113.1, and 39.3 (Figure S33). Anal. calcd. for $C_{18}H_{13}Cl_2N_5O_3S_2$: C, 44.82; H, 2.72; Cl, 14.70; N, 14.52; O, 9.95; S, 13.29. Found: C, 44.86; H, 2.77; Cl, 14.75; N, 14.58; O, 9.99; S, 13.38.

2-[2,2-Dicyano-1-(3-fluorophenylamino)vinylthio]-N-*(4-sulfamoylphenyl)acetamide (**7l**)*

Yield 80.9%, m.p. 210°C; IR (cm^{-1}): 3,270 ($-NH_2$), 3,200 (–NH), 3,086 (=C–H, aromatic), 2,889 ($-CH_2$, aliphatic), 2,209 (CN), 1,705 (C=O), 1,655 (C=C), 1,322, and 1,152 (S=O; Figure S34); ^{1}H NMR (300 MHz, DMSO-d_6, ppm): 10.6–10.8 (2H, s, –NH), 7.76 (2H, d, =CH, *J* = 8.8 Hz), 7.68 (2H, d, =CH, *J* = 8.8 Hz), 7.0–7.6 (4H, m, =CH), 7.3 (2H, s, $-NH_2$), and 4.1 (2H, s, $-CH_2$; Figure S35); ^{13}C NMR (75 MHz, DMSO-d_6, ppm): 170.2, 166.64, 161.2, 141.9, 139.6, 131.7, 131.6, 127.5, 120, 119.6, 113.9, 113.6, 111.2, 110.9, and 35.4 (Figure S36). Anal. calcd. for $C_{18}H_{14}FN_5O_3S_2$: C, 50.11; H, 3.27; F, 4.4; N, 16.23; O, 11.12; S, 14.86. Found: C, 50.18; H, 3.29; F, 4.47; N, 16.28; O, 11.17; S, 14.89.

2-[2,2-Dicyano-1-(4-fluorophenylamino)vinylthio]-N-*(4-sulfamoylphenyl)acetamide (**7m**)*

Yield 78.5%, m.p. 212°C; IR (cm^{-1}): 3,271 ($-NH_2$), 3,208 (–NH), 3,136 (=C–H, aromatic), 2,988 ($-CH_2$, aliphatic), 2,220 (CN), 1,660 (C=O), 1,622 (C=C), 1,319, and 1,151 (S=O; Figure S37); ^{1}H NMR (300 MHz, DMSO-d_6, ppm): 10.6–10.8 (2H, s, –NH), 7.76 (2H, d, =CH, *J* = 8.7 Hz), 7.69 (2H, d, =CH, *J* = 8.7 Hz), 7.20 (2H, d, =CH, *J* = 8.4 Hz), 7.13 (2H, d, =CH, *J* = 8.3 Hz), 7.3 (2H, s, $-NH_2$), and 4.1 (2H, s, $-CH_2$; Figure S38); ^{13}C NMR (75 MHz, DMSO-d_6, ppm): 170.3, 166.6, 141.9, 139.6, 137.4, 127.5, 127.4, 126.8, 126.7, 119.6, 117, 116.6, and 37.98 (Figure S39). Anal. calcd. for $C_{18}H_{14}FN_5O_3S_2$: C, 50.11; H, 3.27; F, 4.4; N, 16.23; O, 11.12; S, 14.86. Found: C, 50.16; H, 3.29; F, 4.45; N, 16.26; O, 11.19; S, 14.89.

2-[2,2-Dicyano-1-(3-(trifluoromethyl)phenylamino)vinylthio]-N-*(4-sulfamoylphenyl)acetamide (**7n**)*

Yield 68.5%, m.p. 188°C; IR (cm^{-1}): 3,264 ($-NH_2$), 3,200 (–NH), 3,068 (=C–H, aromatic), 2,988 ($-CH_2$, aliphatic), 2,217 (CN), 1,660 (C=O), 1,622 (C=C), 1,330, and 1,150 (S=O; Figure S40); ^{1}H NMR (300 MHz, DMSO-d_6, ppm): 10.6–10.8 (2H, s, –NH), 7.74 (2H, d, =CH, *J* = 8.7 Hz), 7.67 (2H, d, =CH, *J* = 8.6 Hz), 7.4 (4H, m, =CH), 7.3 (2H, s, $-NH_2$), and 4.1 (2H, s, $-CH_2$; Figure S41); ^{13}C NMR (75 MHz, DMSO-d_6, ppm): 170.69, 166.6, 141.9, 139.8, 139.5, 131.2, 130.7, 127.8, 127.4, 126.2, 123.5, 122.6, 120.4, 119.5, 116.6, and 38.2 (Figure S42). Anal. calcd. for $C_{19}H_{14}F_3N_5O_3S_2$: C, 47.4; H, 2.93; F, 11.84; N, 14.55; O, 9.97; S, 13.32. Found: C, 47.44; H, 2.98; F, 11.89; N, 14.58; O, 9.99; S, 13.37.

2-[2,2-Dicyano-1-(4-iodophenylamino)vinylthio]-N-*(4-sulfamoylphenyl)acetamide (**7o**)*

Yield 78.5%, m.p. 213°C; IR (cm^{-1}): 3,264 ($-NH_2$), 3,205 (–NH), 3,136 (=C–H, aromatic), 2,988 ($-CH_2$, aliphatic), 2,219 (CN), 1,660 (C=O), 1,622 (C=C), 1,330, and 1,150 (S=O; Figure S43); ^{1}H NMR (300 MHz, DMSO-d_6, ppm): 10.6–10.8 (2H, s, –NH), 7.75 (2H, d, =CH, *J* = 8.5 Hz), 7.67 (2H, d, =CH, *J* = 8.5 Hz), 7.22 (2H, d, =CH, *J* = 8.1 Hz), 7.00 (2H, d, =CH, *J* = 8.1 Hz), 7.3 (2H, s, $-NH_2$), and 4.1 (2H, s, $-CH_2$; Figure S44); ^{13}C NMR (75 MHz, DMSO-d_6, ppm): 170.1, 166.5, 141.9, 139.5, 139.4, 138.7, 138.6, 127.8, 127.5, 125.9, 119.6, 119.5, and 38.0 (Figure S45). Anal. calcd. for $C_{18}H_{14}IN_5O_3S_2$: C, 40.08; H, 2.62; I, 23.53; N, 19.98; O, 8.9; S, 11.89. Found: C, 40.18; H, 2.65; I, 23.55; N, 20.05; O, 8.94; S, 11.93.

4.2 | Biological studies

4.2.1 | CA activity assay

The chromatography media used in the experiments and all chemical compounds, including 4-nitrophenyl acetate (N8130), were of analytical grade and purchased from Sigma-Aldrich Chemie GmbH (Taufkirchen, Germany). Prestained protein MW standard and markers[59] (26617, a mixture of recombinant proteins ranging from 10 to 180 kDa)[60] were obtained from Thermo Fisher Scientific Inc. (Waltham, MA). AAZ was used as the reference drug. Solutions of all newly synthesized analogs (**7a–o**) and AAZ were prepared in DMSO at an initial concentration of 1 mg/ml. The concentration of DMSO in the final reaction mixture was approximately 1%. CA isoforms (I and II) were obtained with purification from human erythrocytes by Sepharose-4B-L-tyrosine-sulfanilamide affinity chromatography, as in our previous work.[61] The protein concentration of the eluates was determined by a straightforward analytical procedure at 595 nm,[62] according to the Bradford method,[63] spectrophotometrically.[64] The purity of the purified enzyme fractions of both isoenzymes was determined by sodium dodecyl sulfate polyacrylamide gel electrophoresis,[65] which was realized on 8% slab gels,[66] as explained by Laemmli.[67] Esterase activity of human erythrocyte CA isoforms was determined by following the change in absorbance at 348 nm over a period of 3 min at 25°C, according to the method defined by Verpoorte et al.[68] All rate measurements were conducted in triplicate. IC_{50} and K_I values were computed as in our previous work.[69] The inhibition type for each of the derivatives was found using Lineweaver–Burk curves.[70]

4.2.2 | AChE activity assay

Acetylcholinesterase from *Electrophorus electricus* (C2888, Type V-S), which is a tetramer composed of four equal subunits of 70 kDa each, 5,5′-dithiobis(2-nitrobenzoic acid) (D8130, DTNB), and acetylthiocholine iodide (01480, AChI) were acquired from Sigma-Aldrich Chemie GmbH (Taufkirchen, Germany). In vitro effects on AChE activity of the target derivatives (**7a–o**) were evaluated by the method of Ellman et al.[71] TAC was used as the reference drug. All the measurements were repeated three times.

4.3 | In silico studies

4.3.1 | ADMET study

Qikprop software,[72] contained in the Schrodinger Suite 2019-3, was used to predict pharmaceutically relevant and varied ADMET and drug-likeness parameters of the synthesized ketene *N,S*-acetal sulfonamides (**7a–o**), such as water/gas partition coefficient (QPlogPw), octanol/water partition coefficient (QPlogPo/w), aqueous solubility (QPlogS), skin permeability (QPlogKp), brain/blood partition coefficient (QPlogBB), human serum albumin-binding (QPlogKhsa), IC_{50} value for blockage of HERG K^+ channels (QPlogHERG), human oral absorption (HOA), the van der Waals surface area of polar nitrogen and oxygen atoms (PSA), the number of violations of Lipinski's rule of five,[73] and the number of violations of Jorgensen's rule of three,[74] which are significant in the novel drug discovery and development process.

4.3.2 | Molecular docking study

The crystal structures of the receptors, including *h*CA I (5E2M, resolution 1.41 Å, complex with V14),[75] *h*CA II (6H29, resolution 1.46 Å, complex with FK8),[76] and AChE (4M0E, resolution 2.00 Å, complex with 1YL),[77] which are downloaded from the RCSB PDB (rcsb.org),[78] were prepared using the Protein Preparation Wizard[79] in Schrödinger Suite 2019-3. OPLS3e force field[80] was used for the optimization of both the synthesized ketene *N,S*-acetal sulfonamide analogs (**7a–o**) and the receptors. The grid box accounting for the binding site residues of *h*CA isoforms I, II, and AChE was generated[81] by the Receptor Grid Generation module.[82] Three-dimensional ligand structures were prepared by the LigPrep tool[83] and implemented for their minimization states at neutral pH (7.0 ± 0.5) with Epik.[84] Extra precision Glide protocol[85] in Schrödinger Suite[86] was performed and bioactive compound structures were treated as flexible to obtain five poses for each ligand. The Prime MM–GBSA module[87] (Schrödinger Release 2019-3) using the VSGB solvent model[88] and OPLS3e force field[89] was applied to calculate the binding free energy (ΔG Bind) of the synthesized derivatives (**7a–o**) toward the receptors (5E2M, 6H29, and 4M0E).

4.4 | Statistical studies

The analysis of the data and drawing of graphs were realized using GraphPad Prism version 6 for Mac, GraphPad Software, La Jolla, CA. Also, K_I constants were determined using SigmaPlot version 12, from Systat Software, San Jose, CA. The results were exhibited as mean ± standard deviation (95% confidence intervals). Differences between data sets were considered as statistically significant when the p value was <0.05.

ACKNOWLEDGMENTS

This study was supported by the Research Fund of Erzincan Binali Yıldırım University (Grant number FBA-2017-501), the Research Fund of Sakarya University (Grant number 2016-02-04–018), and the Research Fund of Anadolu University (Grant number 1610S681).

CONFLICT OF INTERESTS

The authors declare that there are no conflicts of interests.

ORCID

Cüneyt Türkeş http://orcid.org/0000-0002-2932-2789

REFERENCES

[1] L. Zhang, J. Dong, X. Xu, Q. Liu, *Chem. Rev.* **2016**, *116*, 287. https://doi.org/10.1021/acs.chemrev.5b00360
[2] M. Yokoyama, H. Togo, S. Kondo, *Sulfur Rep.* **1990**, *10*, 23. https://doi.org/10.1080/01961779008048749
[3] E. I. Al-Afaleq, *Synth. Commun.* **2001**, *31*, 3557. https://doi.org/10.1081/SCC-100106218
[4] N. Berber, *Sakarya University J. Sci.* **2019**, *23*, 554. https://doi.org/10.16984/saufenbilder.414310
[5] F. El-Baih, H. Al-Blowy, H. Al-Hazimi, *Molecules* **2006**, *11*, 498. https://doi.org/10.3390/11070498
[6] G. Sommen, A. Comel, G. Kirsch, *Tetrahedron* **2003**, *59*, 1557. https://doi.org/10.1016/S0040-4020(03)00054-1
[7] K. S. Jain, S. K. Chaudhari, N. S. More, K. D. More, S. A. Wakedkar, M. K. Kathiravan, *Int. J. Org. Chem.* **2011**, *1*, 47. https://doi.org/10.4236/ijoc.2011.12009
[8] H. Mukaiyama, T. Nishimura, H. Shiohara, S. Kobayashi, Y. Komatsu, S. Kikuchi, E. Tsuji, N. Kamada, H. Ohnota, H. Kusama, *Chem. Pharmacol. Bull.* **2007**, *55*, 881. https://doi.org/10.1248/cpb.55.881
[9] W. Fischer, R. Bodewei, G. Satzinger, *Naunyn-Schmiedeberg's Arch. Pharm.* **1992**, *346*, 442. https://doi.org/10.1007/BF00171088
[10] M. Tomizawa, D. L. Lee, J. E. Casida, *J. Agric. Food Chem.* **2000**, *48*, 6016. https://doi.org/10.1021/jf000873c
[11] P. Jeschke, R. Nauen, M. E. Beck, *Angew. Chem. Int. Ed.* **2013**, *52*, 9464. https://doi.org/10.1002/anie.201302550
[12] X. Fei, Y. Gu, Y. Ban, Z. Liu, B. Zhang, *Bioorg. Med. Chem.* **2009**, *17*, 585. https://doi.org/10.1016/j.bmc.2008.11.083
[13] W. E. Evenson, L. M. Boden, K. A. Muzikar, D. J. O'Leary, *J. Org. Chem.* **2012**, *77*, 10967. https://doi.org/10.1021/jo3021659
[14] R. Cremlyn, *An Introduction to Organosulfur Chemistry*, John Wiley and Sons, New York, NY **1996**.
[15] N. Anand, W. A. Remers, *Burger's Med. Chem. Drug Discov.* **2003**, 481. https://doi.org/10.1002/0471266949.bmc086.pub2
[16] C. O. Wilson, O. Gisvold, J. H. Block, J. M. Beale, *Wilson and Gisvold's Textbook of Organic Medicinal and Pharmaceutical Chemistry*, (Eds: J. H. Block, J. M. Beale, Jr.), Lippincott Williams & Wilkins, Philadelphia, PA **2004**.
[17] A. Scozzafava, M. D. Banciu, A. Popescu, C. T. Supuran, *J. Enzyme Inhib.* **2000**, *15*, 443. https://doi.org/10.3109/14756360009040700
[18] D. Aggarwal, A. Garg, I. P. Kaur, *J. Pharm. Pharmacol.* **2004**, *56*, 1509. https://doi.org/10.1211/0022357044896
[19] C. Van Kesteren, J. H. Beijnen, J. H. M. Schellens, *Anti-Cancer Drugs* **2002**, *13*, 989. https://doi.org/10.1097/00001813-200211000-00002
[20] J. Drews, *Science* **2000**, *287*, 1960. https://doi.org/10.1126/science.287.5460.1960
[21] W. J. Moree, L. C. van Gent, G. A. van der Marel, R. M. J. Liskamp, *Tetrahedron* **1993**, *49*, 1133. https://doi.org/10.1016/S0040-4020(01)86293-1
[22] A. Scozzafava, T. Owa, A. Mastrolorenzo, C. T. Supuran, *Curr. Med. Chem.* **2003**, *10*, 925. https://doi.org/10.2174/0929867033457647
[23] T. H. Maren, *Physiol. Rev.* **1967**, *47*, 595. https://doi.org/10.1152/physrev.1967.47.4.595
[24] T. Wroblewski, A. Graul, J. Castaner, *Drugs Future* **1998**, *23*, 365.
[25] F. C. Novello, J. M. Sprague, *J. Am. Chem. Soc.* **1957**, *79*, 2028. https://doi.org/10.1021/ja01565a079
[26] J. H. Jones, J. V. Jones, *Br. Med. J.* **1959**, *2*, 928. https://doi.org/10.1136/bmj.2.5157.928
[27] S. Y. P'an, A. Scriabine, D. E. McKersie, W. M. McLamore, *J. Pharmacol. Exp. Ther.* **1960**, *128*, 122.
[28] A. A. Rubin, F. E. Roth, M. M. Winbury, J. G. Topliss, M. H. Sherlock, N. Sperber, J. Black, *Science* **1961**, *133*, 2067. https://doi.org/10.1126/science.133.3470.2067
[29] M. Klapper, L. E. O. Richard, *South. Med. J.* **1962**, *55*, 297. https://doi.org/10.1097/00007611-196203000-00018
[30] F. Topal, *Int. J. Food Prop.* **2019**, *22*, 583. https://doi.org/10.1080/10942912.2019.1597882
[31] J. M. Roldán-Peña, V. Romero-Real, J. Hicke, I. Maya, A. Franconetti, I. Lagunes, J. M. Padrón, S. Petralla, E. Poeta, M. Naldi, *Eur. J. Med. Chem.* **2019**, *181*, 111550. https://doi.org/10.1016/j.ejmech.2019.07.053
[32] D. G. van Greunen, C. J. van der Westhuizen, W. Cordier, M. Nell, A. Stander, V. Steenkamp, J.-L. Panayides, D. L. Riley, *Eur. J. Med. Chem.* **2019**, *179*, 680. https://doi.org/10.1016/j.ejmech.2019.06.088
[33] M. Topal, *Int. J. Food Prop.* **2019**, *22*, 1527. https://doi.org/10.1080/10942912.2019.1656234
[34] A. Kuppusamy, M. Arumugam, S. George, *Int. J. Biol. Macromol.* **2017**, *95*, 199. https://doi.org/10.1016/j.ijbiomac.2016.11.062
[35] F. Vafadarnejad, E. Karimpour-Razkenari, B. Sameem, M. Saeedi, O. Firuzi, N. Edraki, M. Mahdavi, T. Akbarzadeh, *Bioorg. Chem.* **2019**, *92*, 103192. https://doi.org/10.1016/j.bioorg.2019.103192
[36] M. M. Mesulam, A. Guillozet, P. Shaw, A. Levey, E. G. Duysen, O. Lockridge, *Neuroscience* **2002**, *110*, 627. https://doi.org/10.1016/S0306-4522(01)00613-3
[37] M. Topal, *Rec. Nat. Prod.* **2019**, *14*, 129. https://doi.org/10.25135/rnp.155.19.06.1326
[38] C. de los Ríos, J. Marco-Contelles, *Eur. J. Med. Chem.* **2019**, *166*, 381. https://doi.org/10.1016/j.ejmech.2019.02.005
[39] S. Ghobadi, M. R. Ashrafi-Kooshk, H. Mahdiuni, R. Khodarahmi, *Int. J. Biol. Macromol.* **2018**, *108*, 240. https://doi.org/10.1016/j.ijbiomac.2017.12.011
[40] C. Çağlayan, P. Taslimi, Y. Demir, S. Küçükler, F. M. Kandemir, İ. Gulçin, *J. Biochem. Mol. Toxicol.* **2019**, *33*, e22381. https://doi.org/10.1002/jbt.22381
[41] L. Vats, R. Kumar, S. Bua, A. Nocentini, P. Gratteri, C. T. Supuran, P. K. Sharma, *Eur. J. Med. Chem.* **2019**, *183*, 111698. https://doi.org/10.1016/j.ejmech.2019.111698
[42] A. Nocentini, S. M. Osman, S. Del Prete, C. Capasso, Z. A. Alothman, C. T. Supuran, *Bioorg. Chem.* **2019**, *93*, 103336. https://doi.org/10.1016/j.bioorg.2019.103336
[43] A. Zakšauskas, E. Čapkauskaitė, L. Jezepčikas, V. Linkuvienė, V. Paketurytė, A. Smirnov, J. Leitans, A. Kazāks, E. Dvinskis, E. Manakova, *Eur. J. Med. Chem.* **2019**, *185*, 111825. https://doi.org/10.1016/j.ejmech.2019.111825
[44] A. Maharramov, R. Kaya, P. Taslimi, M. Kurbanova, A. Sadigova, V. Farzaliyev, A. Sujayev, İ. Gulçin, *Arch. Pharm.* **2019**, *352*, 1800317. https://doi.org/10.1002/ardp.201800317
[45] A. Topal, M. Atamanalp, E. Oruç, Y. Demir, Ş. Beydemir, A. Işık, *Arch. Ind. Hygiene Toxicol.* **2014**, *65*, 377. https://doi.org/10.2478/10004-1254-65-2014-2547
[46] H. G. Bilgicli, P. Taslimi, B. Akyuz, B. Tuzun, I. Gulcin, *Arch. Pharm.* **2020**, *353*, e1900304. https://doi.org/10.1002/ardp.201900304
[47] F. Turkan, A. Cetin, P. Taslimi, H. S. Karaman, İ. Gulçin, *Arch. Pharm* **2019**, *352*, e1800359. https://doi.org/10.1002/ardp.201800359
[48] F. Topal, *J. Biochem. Mol. Toxicol.* **2019**, *33*, e22385. https://doi.org/10.1002/jbt.22385
[49] D. Tanini, A. Capperucci, M. Ferraroni, F. Carta, A. Angeli, C. T. Supuran, *Eur. J. Med. Chem.* **2019**, *185*, 111811. https://doi.org/10.1016/j.ejmech.2019.111811
[50] M. A. Said, W. M. Eldehna, A. Nocentini, A. Bonardi, S. H. Fahim, S. Bua, D. H. Soliman, H. A. Abdel-Aziz, P. Gratteri, S. M. Abou-Seri, *Eur. J. Med. Chem.* **2019**, *185*, 111843. https://doi.org/10.1016/j.ejmech.2019.111843
[51] V. Alterio, A. Di Fiore, K. D'Ambrosio, C. T. Supuran, G. de Simone, *Chem. Rev.* **2012**, *112*, 4421. https://doi.org/10.1021/cr200176r
[52] L. Kelebekli, N. Balcı, E. Şahin, *Tetrahedron* **2014**, *70*, 5175. https://doi.org/10.1016/j.tet.2014.05.101
[53] U. Atmaca, S. Daryadel, P. Taslimi, M. Çelik, İ. Gülçin, *Arch. Pharm.* **2019**, *352*, e1900200. https://doi.org/10.1002/ardp.201900200

[54] S. Kılıcaslan, M. Arslan, Z. Ruya, Ç. Bilen, A. Ergün, N. Gençer, O. Arslan, *J. Enzyme Inhib. Med. Chem.* **2016**, *31*, 1300. https://doi.org/10.3109/14756366.2015.1128426
[55] E. M. Duffy, W. L. Jorgensen, *J. Am. Chem. Soc.* **2000**, *122*, 2878. https://doi.org/10.1021/ja993663t
[56] C. A. Lipinski, F. Lombardo, B. W. Dominy, P. J. Feeney, *Adv. Drug Del. Rev.* **1997**, *23*, 3. https://doi.org/10.1016/S0169-409X(96)00423-1
[57] C. Türkeş, M. Arslan, Y. Demir, L. Çoçaj, A. R. Nixha, Ş. Beydemir, *Bioorg. Chem.* **2019**, *89*, 103004. https://doi.org/10.1016/j.bioorg.2019.103004
[58] M. Ahmed, M. A. Qadir, A. Hameed, M. N. Arshad, A. M. Asiri, M. Muddassar, *Bioorg. Chem.* **2018**, *76*, 218. https://doi.org/10.1016/j.bioorg.2017.11.015
[59] C. Türkeş, Y. Demir, Ş. Beydemir, *App. Biochem. Biotechnol.* **2019**, *189*, 318. https://doi.org/10.1007/s12010-019-03009-x
[60] Y. Demir, C. Türkeş, Ş. Beydemir, *Anti-Cancer Agents Med. Chem.* **2020**, *20*. https://doi.org/10.2174/1871520620666200218110645 PMID: 32067621.
[61] H. E. Aslan, Y. Demir, M. S. Özaslan, F. Türkan, Ş. Beydemir, Ö. I. Küfrevioğlu, *Drug Chem. Toxicol.* **2019**, *42*, 634. https://doi.org/10.1080/01480545.2018
[62] C. Türkeş, H. Söyüt, Ş. Beydemir, *Open J. Biochem.* **2013**, *1*, 10. https://doi.org/10.15764/BIOC.2014.01002
[63] Y. Akbaba, C. Türkeş, L. Polat, H. Söyüt, E. Şahin, A. Menzek, S. Göksu, Ş. Beydemir, *J. Enzyme Inhib. Med. Chem.* **2013**, *28*, 1073. https://doi.org/10.3109/14756366.2012.715287
[64] M. M. Bradford, *Anal. Biochem.* **1976**, *72*, 248. https://doi.org/10.1016/0003-2697(76)90527-3
[65] C. Türkeş, H. Söyüt, Ş. Beydemir, *Pharmacol. Rep.* **2014**, *66*, 74. https://doi.org/10.1016/j.pharep.2013.08.007
[66] C. Türkeş, Y. Demir, Ş. Beydemir, *J. Biomol. Struct. Dyn.* **2020**, 1. https://doi.org/10.1080/07391102.2020.1736631
[67] U. K. Laemmli, *Nature* **1970**, *227*, 680. https://doi.org/10.1038/227680a0
[68] J. A. Verpoorte, S. Mehta, J. T. Edsall, *J. Biol. Chem.* **1967**, *242*, 4221.
[69] C. Türkeş, H. Söyüt, Ş. Beydemir, *J. Enzyme Inhib. Med. Chem.* **2015**, *30*, 622. https://doi.org/10.3109/14756366.2014.959511
[70] C. Türkeş, H. Söyüt, Ş. Beydemir, *Environ. Toxicol. Pharmacol.* **2016**, *42*, 252. https://doi.org/10.1016/j.etap.2015.11.024
[71] G. L. Ellman, K. D. Courtney, V. Andres Jr, R. M. Featherstone, *Biochem. Pharmacol.* **1961**, *7*, 88. https://doi.org/10.1016/0006-2952(61)90145-9
[72] B. N. Sağlık, U. A. Çevik, D. Osmaniye, S. Levent, B. K. Çavuşoğlu, Y. Demir, S. Ilgın, Y. Özkay, A. S. Koparal, Ş. Beydemir, *Bioorg. Chem.* **2019**, *91*, 103153. https://doi.org/10.1016/j.bioorg.2019.103153
[73] M. Işık, Ş. Beydemir, Y. Demir, M. Durgun, C. Türkeş, A. Nasır, A. Necip, M. Akkuş, *Int. J. Biol. Macromol.* **2020**, *146*, 1111. https://doi.org/10.1016/j.ijbiomac.2019.09.237
[74] S. Gündoğdu, C. Türkeş, M. Arslan, Y. Demir, Ş. Beydemir, *ChemistrySelect* **2019**, *4*, 13347. https://doi.org/10.1002/slct.201903458
[75] A. Zubrienė, A. Smirnov, V. Dudutienė, D. D. Timm, J. Matulienė, V. Michailovienė, A. Zakšauskas, E. Manakova, S. Gražulis, D. Matulis, *ChemMedChem* **2017**, *12*, 161. https://doi.org/10.1002/cmdc.201600509
[76] G. Simone, S. MariaáMonti, *Chem. Commun.* **2018**, *54*, 10312. https://doi.org/10.1039/C8CC05755A
[77] J. Cheung, E. N. Gary, K. Shiomi, T. L. Rosenberry, *ACS Med. Chem. Lett.* **2013**, *4*, 1091. https://doi.org/10.1021/ml400304w
[78] C. Türkeş, *J. Inst. Sci. Technol.* **2019**, *9*, 1013. https://doi.org/10.21597/jist.491054
[79] M. Işık, *Neurochem. Res.* **2019**, *44*, 2147. https://doi.org/10.1007/s11064-019-02852-y
[80] C. Türkeş, *Protein Pept. Lett.* **2019**, *26*, 392. https://doi.org/10.2174/0929866526666190226162225
[81] C. Türkeş, Ş. Beydemir, *App. Biochem. Biotechnol.* **2020**, *190*, 252. https://doi.org/10.1007/s12010-019-03073-3
[82] M. Işık, Y. Demir, M. Durgun, C. Türkeş, A. Necip, Ş. Beydemir, *Chem. Pap.* **2019**, *74*, 1. https://doi.org/10.1007/s11696-019-00988-3.
[83] Ş. Beydemir, C. Türkeş, A. Yalçın, *Drug Chem. Toxicol.* **2019**, 1. https://doi.org/10.1080/01480545.2019.1620266
[84] S. Kalinin, A. Nocentini, A. Kovalenko, V. Sharoyko, A. Bonardi, A. Angeli, P. Gratteri, T. B. Tennikova, C. T. Supuran, M. Krasavin, *Eur. J. Med. Chem.* **2019**, *182*, 111642. https://doi.org/10.1016/j.ejmech.2019.111642
[85] C. Türkeş, *J. Pharm. Pharmacol.* **2019**, *71*, 1553. https://doi.org/10.1111/jphp.13141
[86] C. Türkeş, Ş. Beydemir, Ö. İ. Küfrevioğlu, *ChemistrySelect* **2019**, *4*, 9731. https://doi.org/10.1002/slct.201902424
[87] A. Ece, *J. Biomol. Struct. Dyn.* **2019**, *38*, 1. https://doi.org/10.1080/07391102.2019.1583606
[88] P. Mehta, S. Srivastava, M. Sharma, I. Singh, R. Malik, *Int. J. Biol. Macromol.* **2018**, *119*, 1113. https://doi.org/10.1016/j.ijbiomac.2018.08.032
[89] P. Sharma, A. Tripathi, P. N. Tripathi, S. K. Prajapati, A. Seth, M. K. Tripathi, P. Srivastava, V. Tiwari, S. Krishnamurthy, S. K. Shrivastava, *Eur. J. Med. Chem.* **2019**, *167*, 510. https://doi.org/10.1016/j.ejmech.2019.02.030

SUPPORTING INFORMATION

Additional supporting information may be found online in the Supporting Information section.

How to cite this article: Istrefi Q, Türkeş C, Arslan M, et al. Sulfonamides incorporating ketene *N*,*S*-acetal bioisosteres as potent carbonic anhydrase and acetylcholinesterase inhibitors. *Arch Pharm*. 2020;e1900383. https://doi.org/10.1002/ardp.201900383